Journal of Volcanology and Geothermal Research 255 (2013) 43–56

Contents lists available at SciVerse ScienceDirect

Journal of Volcanology and Geothermal Research

journal homepage: www.elsevier.com/locate/jvolgeores

Morphometrical and geochronological constraints on the youngest eruptive activity in East-Central Europe at the Ciomadul (Csomád) lava dome complex, East Carpathians

Dávid Karátson [a,*], Tamás Telbisz [a], Szabolcs Harangi [b], Enikő Magyari [c], István Dunkl [d], Balázs Kiss [b], Csaba Jánosi [e], Daniel Veres [f,g], Mihály Braun [h], Emőke Fodor [a], Tamás Biró [a], Szabolcs Kósik [a], Hilmar von Eynatten [d], Ding Lin [i]

[a] Eötvös University, Department of Physical Geography, H-1117 Budapest, Pázmány s. 1/C, Hungary
[b] Eötvös University, Department of Petrology and Geochemistry, H-1117 Budapest, Pázmány s. 1/C, Hungary
[c] Hungarian Natural History Museum, Paleonthological Research Group, Hungarian Academy of Sciences, P.O. Box 222, H-1476 Budapest, Hungary
[d] University of Göttingen, Geoscience Center, Department of Sedimentology & Environmental Geology, Goldschmidtstr, 3, D-37077, Göttingen, Germany
[e] 530225 Miercurea Ciuc, str. Inimii 3/14, Romania
[f] Faculty of Environmental Science and Engineering, Babes-Bolyai University, Fantanele 30, 400294 Cluj-Napoca, Romania
[g] Romanian Academy, Institute of Speleology, Clinicilor 5, 400006 Cluj-Napoca, Romania
[h] Department of Inorganic and Analytical Chemistry, A18 University of Debrecen, P.O. Box 21, H-4010 Debrecen, Hungary
[i] Institute of Tibetan Plateau Research and Institute of Geology and Geophysics, Chinese Academy of Sciences, Beijing 100029, China

ARTICLE INFO

Article history:
Received 21 April 2012
Accepted 23 January 2013
Available online 31 January 2013

Keywords:
Lava dome morphometry
DEM analysis
Carpathian volcanism
U–Pb and (U–Th)/He geochronology
Paleolimnology

ABSTRACT

The timing of Late Pleistocene volcanic activity of the Ciomadul (Csomád) dacitic lava dome complex, site of the youngest eruptions in the Carpathians, has been constrained by morphometric analysis and radiometric chronology. Peléan domes and asymmetric domes/coulées built up the volcano, including the central edifice that hosts the youngest twin craters of Mohoş (Mohos) peat bog and lake St. Ana (Szent Anna). A comparative digital elevation model (DEM)-based morphometric analysis of lava domes (29 worldwide examples including 5 domes from Ciomadul) shows that it is the mean slope of the upper dome flank that correlates best with age. Although the logarithmic relationship is only moderately strong (R = 0.80), slope characteristics of the Ciomadul domes fit to those of 10–100 ka old domes. These young ages contradict the previous K/Ar dates giving as old as 1 Ma ages on a number of domes, but are supported by ongoing U–Pb and (U–Th)/He zircon dating. The latter methods constrain the whole volcanic activity to the past 250 ka and the emplacement of most lava domes within the period of 150–100 ka.

The volcanism at Ciomadul produced alternating effusive and explosive eruptions including lava dome collapses and successive crater formations. The latest, possibly subplinian explosive event formed the well-preserved St. Ana crater. Radiocarbon dating of organic remains from a sediment core that reached 11 m into the lacustrine infill of St. Ana suggests that the crater was formed prior to 26,000 years BP.

1. Introduction

It has long been known that the final eruptive activity in East-Central Europe occurred at the Ciomadul (Csomád)[1] volcano in the East Carpathians, Romania, in the Late Quaternary (Peltz, 1971; Boccaletti et al., 1973; Peltz et al., 1987), extending the volcanic activity of the Carpathian Volcanic Arc to the last glacial stage (late Marine Isotope Stage 3).

The Ciomadul volcano (Fig. 1) is a dacitic lava dome complex consisting of a central edifice truncated by the twin craters of Lake Sfânta [St.] Ana (Szent Anna) and Mohoş (Mohos) peat bog, and surrounded by a number of individual lava domes as well as a narrow volcaniclastic ring plain (Schreiber, 1972; Szakács and Seghedi, 1990, 1995; Popa et al., 2011). On the basis of K/Ar dating as well as ^{14}C dating of chared organic remains (Casta, 1980; Pécskay et al., 1992, 1995; Moriya et al., 1996), Szakács and Seghedi (1990, 1995), and Szakács et al. (2002) suggested that the volcanic activity could be divided into a long-lasting lava-dome growth phase and a final, much shorter explosive phase. However, given methodological problems linked with young K/Ar dates and that such a division is uncommon at dome complexes worldwide (see later), the postulated eruptive scenario as well as its duration call for re-investigation.

In this paper, we address the chronology of the volcanism of Ciomadul using a twofold approach. First, a volcanic landform analysis

* Corresponding author. Tel.: +36 13722500.
E-mail address: dkarat@ludens.elte.hu (D. Karátson).

[1] Official Romanian names are followed by local Hungarian names (in brackets). In the text, official names are used for larger regional features (highest mountains, lakes, towns), and local names for minor features, which is helpful for the reader to find these names on local maps.

0377-0273/$ – see front matter © 2013 Elsevier B.V. All rights reserved.
http://dx.doi.org/10.1016/j.jvolgeores.2013.01.013

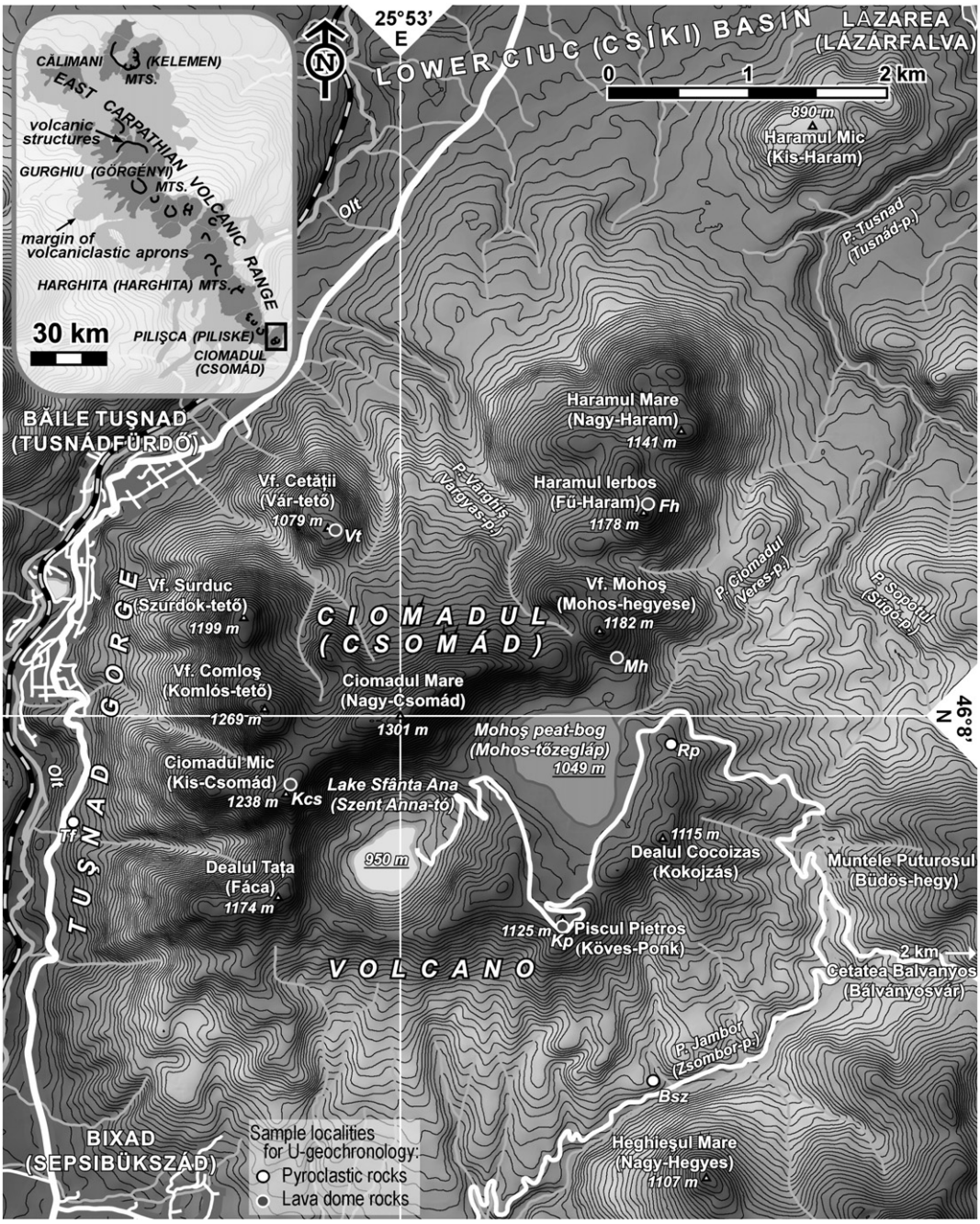

Fig. 1. Geographic setting and topographic names of the Ciomadul (Csomád) volcano. Original map source: Băile Tuşnad şi impremejurimile (Tusnádfürdő és környéke), Discover ECO-Romania, 1:20,000, Nr. 7. Green Steps, Braşov, 2010.

is carried out based on a 10 m-resolution digital elevation model (DEM) obtained from the 1:20,000 scale topographic map. We characterize the morphometry of the Ciomadul lava domes in order to infer their age; for comparison, a number of worldwide lava domes are also included in the analysis.

Second, radiometric constraints are used. We present preliminary results from ongoing U–Pb and (U–Th)/He dating on the Ciomadul lava domes and related pyroclastic rocks. Although the data cannot be used at this stage for determining individual ages, they do provide reliable constrains on the time interval of volcanic activity. Furthermore, a multiproxy investigation of the lacustrine deposits of Lake St. Ana crater including ^{14}C dating is applied in order to constrain the onset of lacustrine sedimentation subsequent to the final explosive eruptions.

2. Geological framework

2.1. Geographical–geological setting and paleogeography

The Ciomadul volcano terminates the 700 km-long Inner Carpathian Volcanic Arc, along which a calc-alkaline andesitic–rhyolitic volcanism took place during the past 20 Ma (e.g. Seghedi et al., 2005; Harangi and Lenkey, 2007; Seghedi and Downes, 2011). In particular, its southern segment – the Călimani (Kelemen)–Gurghiu (Görgényi)–Harghita (Hargita) chain (Fig. 1) – displays a regular time-space migration of volcanic activity, together with a gradual decrease in magma output (Szakács et al., 1993, 1997; Pécskay et al., 1995; Mason et al., 1998; Karátson and Timár, 2005).

Ciomadul, located in the southernmost end of Harghita Mountains, is separated from the 1500–1800 m high main volcanic range by the river Olt at Tuşnad (Tusnád) Gorge (Fig. 1). It comprises a group of mid-elevated hills (highest altitude 1301 m at Ciomadul Mare (Nagy-Csomád) rising above the Lower Ciuc (Csíki) Basin (700 m a.s.l.)). The central part of the volcano hosts the twin craters that are encompassed within the relatively flat summit ridge of Ciomadul Mare in the north (Fig. 2A). This ridge, consisting of coherent lava rocks (interpreted as early-stage lava domes: Szakács and Seghedi, 1996; Popa et al., 2011), makes the central edifice somewhat asymmetric, because it is ~200 m higher than the southern ridge of the craters (composed mostly of pyroclastic deposits). Around the central part, distinct, steep hills with regular, conical morphology (Schreiber, 1972) correspond to individual lava domes.

The chemical composition of the Ciomadul volcanic rocks – both lava dome rocks, and pumices from the pyroclastic deposits – is K-rich dacite (SiO_2 = 63–68 wt.%; K_2O = 3.0–3.5 wt.%: Szakács and Seghedi, 1986; Vinkler et al., 2007; Kiss et al., 2011). The mineral assemblages are also fairly similar: plagioclase, hornblende and biotite are the main phenocryst-sized phases; quartz, clinopyroxene, olivine, orthopyroxene, apatite, sphene, allanite and zircon are less frequent.

The volcanic activity of the Ciomadul volcano started at the southern margin of the Lower Ciuc Basin in a fluvio-lacustrine environment (Bulla, 1948; Kristó, 1957; Fielitz and Seghedi, 2005). The landscape was characterized by the structural graben of the Ciuc Basin, which formed in a regional NNW–SSE striking transtensional fault zone coeval with the adjacent volcanism of the Harghita Mountains (Fielitz and Seghedi, 2005). The basin, hosting primarily a lake, was progressively infilled by clastic deposits, coal intercalations, and volcanic sediments (Kristó, 1957; Mureşan and Szakács, 1998; Fielitz and Seghedi, 2005). The basin infill may have been complete at around the time the Ciomadul volcanism commenced, and when the paleo-Olt river started to drain the basin towards the south (László, 2005). Subsequently, the fluvial downcut of river Olt (Bulla, 1948), as well as the growth and uplift of both Ciomadul and the neighboring and likely older volcanoes (e.g. the adjacent Pilişca [Piliske] edifice, Fielitz and Seghedi, 2005: Fig. 1), have resulted in at least four main river terraces clearly visible in and around the Tuşnad Gorge (Bulla, 1948). At a location south of Malnaş (Málnás) village (10 km to the S of Bixad [Sepsibükszád] village, Fig. 1; Bulla, 1948), volcanic "bombs" were first reported by Cholnoky (1943) with reference to pers. commun. with Lajos Lóczy, particularly in the third terrace that can be traced at 14–27 m above the riverbed. Although it is not yet clear if these findings are primary fallout products or reworked material, their presence within the young fluvial terrace deposits is very important. Noteworthy, 25 km to the south of Bixad, near the town of Sfântu Georghe (Sepsiszentgyörgy), Necea (2010) determined an age of 59 ± 6 ka for the third terrace level, and 130 ± 12 ka for the fourth using infrared stimulated luminescence (IRSL) dating.

Currently, the Ciomadul volcanic system is characterized by high heat flux, microseismicity, and intense CO_2 degassing in mofettas around the volcano (Szakács et al., 2002; Vaselli et al., 2002). These features point to a period of dormancy or reflect the cooling of the still existing magma body. In fact, new seismic tomography data

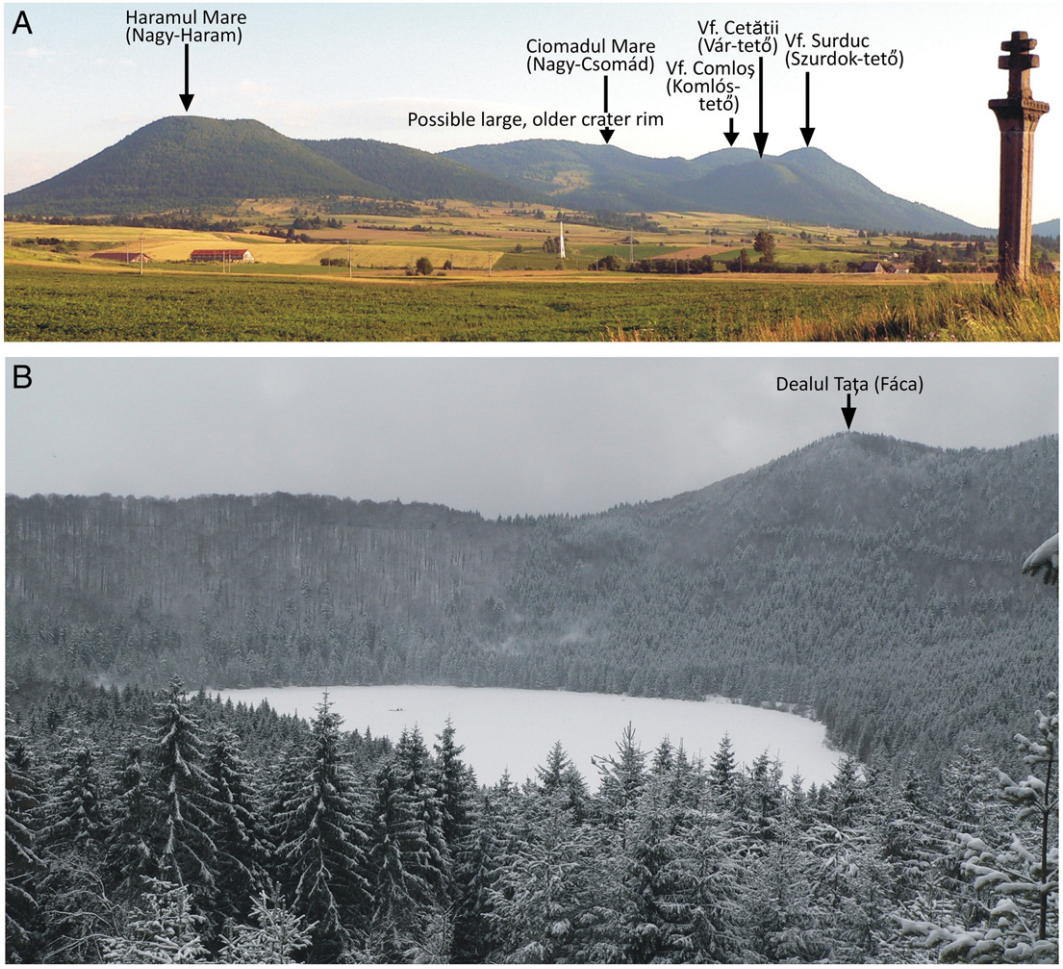

Fig. 2. A — Panoramic view of the Ciomadul (Csomád) massif from the NW. B — View of Lake Sf. Ana (Szent Anna) in winter from the E (the direction of Mohos).

support an active crustal magma chamber 8–20 km underneath (Popa et al., 2011). Given these facts, Ciomadul could be considered a geologically alive volcano, unique in East-Central Europe.

2.2. Current knowledge on the youngest eruptive activity and the origin of volcano morphology

The present knowledge on the volcanism of the Ciomadul is largely based on the pioneering volcanological studies of Szakács and Seghedi (1990, 1995), who suggested that following a massive lava dome effusive phase, explosive eruptions created its two well-preserved craters and produced widespread tephra. Prior to the advent of radiometric dating, a tentative Late Pleistocene age was suggested for this final explosive phase based on local stratigraphic constraints such as the above-discussed lava "bombs" in river terraces and tuff intercalations within Quaternary deposits (Cholnoky, 1922; Bulla, 1948; Peltz, 1971; Szakács and Seghedi, 1990). Tentative geomorphological observations included the "fresh-looking" shape of the craters and lava domes (Cholnoky, 1943; Székely, 1957), and the fact that the central domes are cut by subsequent, regular, closed contours of the two craters (Fig. 1; Karátson, 1994; Kristó, 1995).

Sf. Ana is the only primary open-water crater lake in East-Central Europe (Figs. 1 and 2B). The highly symmetric shape and dimensions of the crater (~1600 m diameter, ~200 m depth) resemble to the large explosion craters such as at Mt. Herbert, Aleutians (Myers, 1992) or at El Chichón, Mexico (Macías et al., 2008). In fact, the deep, intact crater and the very steep inner crater slopes (up to 38° on the northern wall) imply one or more explosive eruptions directly related to the crater morphology.

The older age of the Mohos crater relative to the still existing crater lake of Sf. Ana is evidenced by the facts that it is completely filled in by sediments and a 10 m-thick peat bog (Juvigné et al., 1994; Tantau et al., 2003), and that its western rim is cut by the Sf. Ana crater (Karátson, 1994). The timing of its formation is not known, but an approximate age of ~200 ka was inferred on the basis of K/Ar radiometric dating on neighboring lava dome rocks (Szakács and Seghedi, 1996; Szakács et al., 2002).

Pumice-rich pyroclastic deposits occasionally containing abundant dacitic lithoclasts are widespread on the W, S and NE flank of the central edifice, and are generally attributed to the final crater-forming eruptions (e.g. Szakács and Seghedi, 1996). Direct radiometric dating on these deposits has not yet been performed; however, charcoal and charred wood fragments from pyroclastic deposits were dated at 45–30 ka through the ^{14}C method (Moriya et al., 1996; Harangi et al., 2010; for details, see Section 4.1). With respect to the earlier history of the older Mohos crater, Karátson (2007) and Vinkler et al. (2007) documented a series of pyroclastic-flow and -fall deposits at the crater outlet. These are overlain by tens of volcanogenic sandy–clayey layers (Karátson, 2007) that in turn are overlain by the Holocene peat bog. These findings suggest a significantly long time frame for a former Mohos crater lake evolution. As for St. Ana crater, on the basis of the 45–30 ka radiocarbon age of the final eruptions and the Holocene sedimentary infill (Magyari et al., 2009 and references therein), a similar, albeit possibly shorter evolution is likely.

3. Lava dome morphometry

3.1. Morphology and types of lava domes, and characterization of the Ciomadul domes

Among elementary volcanic landforms, lava domes show one of the highest variability ranging from very small (10 m) to large (1000 m) edifices with simple, symmetric to highly irregular morphologies. Blake (1990) established four main categories characterized by progressively lower height (H) vs diameter (D) ratio: upheaved plug, Peléan dome, coulée and low dome, which the author related to decreasing yield strength of lava. Fink and Griffiths (1998) and Fink and Anderson (2000) also distinguished the "lobate" dome, a variation of Peléan dome, and the "platy" dome, whose folded/fractured surface is eventually broken into plate-like parts.

The shape as well as the eruptive behavior of a growing lava dome is controlled by the way the lava solidifies (e.g. Zimbelman et al., 2000). For example, viscous Peléan domes, in addition to lava extrusion and spreading, may frequently collapse resulting in block-and-ash flows (e.g. Mount Pelée, Martinique, Lesser Antilles; Unzen, Kyushu, Japan; Puy-de-Dôme, Auvergne, France). The main factors determining the final morphology include chemical composition, viscosity and yield strength of magma (Fink and Anderson, 2000; Lyman et al., 2004) as well as the effusive rate, eruption duration, thickness/size of dome, crystal and fluid content, cooling rate, and inclination of the underlying slope (de Silva et al., 1994; Anderson et al., 1995; Fink and Bridges, 1995; Stasiuk and Jaupart, 1997; Watts et al., 2002; Lyman et al., 2004; Hale and Wadge, 2008). The fact that chemical composition is not the only factor is clearly exemplified by the Mt. St. Helens dacitic dome growth between 1980 and 1986 producing both Peléean and low dome shapes (Zimbelman et al., 2000).

The variety of the above control factors might be the reason that the morphometric characterization of lava domes is only tentative. Roughly, lava domes are distinguished from lava flows by an H/D ratio greater than 0.1 (Moriya, 1978; Stasiuk and Jaupart, 1997). A type example, Puy-de-Dôme, has a ratio of 0.22 (Shields, 2010). Aguirre-Díaz et al. (2006) found that the andesitic to dacitic Peléan domes, coulées and low domes (21 studied examples) in the Valle de Bravo volcanic field, Mexico, have H/D ratios 0.17, 0.18 and 0.09, respectively.

However, due to the typically complex shape, inferring the age of a dome should not rely solely on the H/D ratio, even though it works quite well for scoria cones (Wood, 1980; Favalli et al., 2009; Fornaciai et al., 2012). Given the variable width of domes and dome summits, the slope characteristics of the flanks may provide a better approximation for constraining the age of a lava dome. In our study, we postulate that (1) the upper flank slope angles of young lava domes are similar for a given type of shape (in this study, for Peléan domes and steep coulées), and (2) that the upper flank slope values decrease with time due to erosion, similarly to the evolution of other volcano landforms. The validity of these assumptions is evaluated in the Discussion in the light of the results. In order to make our approach statistically reliable, we compared the Ciomadul domes' slope characteristics to those of 24 worldwide lava domes (see next section).

The dacitic Ciomadul lava domes are prominent landforms (Figs. 1 and 2A). Although their small-scale surface features have been eroded (the present climate is temperate with 800–1000 mm annual rainfall), their large-scale shape is relatively well-preserved. Precise identification of individual dome boundaries is difficult due to the overlapping, the erosion-produced aprons, and the erosional downcutting by the Tuşnad Gorge. By contrast, most domes still have undissected flanks and linear slope profiles (especially in the upper part: see Fig. 2A) apparently preserving the primary morphology.

The Ciomadul domes reach 300–400 m height and 1–2 km width (i.e. a ~0.2 H/D ratio) with well-defined, steep upper flanks in most cases, although extremely steep slopes and "pancake" shapes are missing. Therefore, spines/plugs and low domes can be excluded as the original shape, with an exception, the northernmost Haramul Mic (Kis-Haram), which is rather a low dome having much smaller elevation and more gentle slopes (Fig. 1). In the case of Haramul Mare (Nagy-Haram), Haramul Ierbos (Fű-Haram) and Vf. Cetăţii (Vár-tető), the symmetric shape is characteristic of a Peléan dome, whereas the other domes facing the Olt (Vf. Comloş [Komlós-tető] and Vf. Surduc [Szurdok-tető]) are asymmetric domes/coulées superimposed on the westward-dipping slope of the central dome complex (Fig. 1). Some domes having one (typically broad) summit are simple (e.g. Vár-tető, Nagy-Haram); others are lobate (e.g. Fű-Haram). However, even simple

domes (e.g. Nagy-Haram) may have been fed by more than one eruptive vent (e.g. Szakács and Seghedi, 1990). We note that, as well as Kis-Haram, Heghieşul Mare (Nagy-Hegyes), an andesitic dome, and Muntele Puturosul (Büdös-hegy), a dacitic (crypto)dome that cuts through Cretaceous flysch (Szakács and Seghedi, 1986; Fig. 1), were not included in our study, either.

3.2. Obtaining characteristic slope values from DEM analysis

The selection of lava domes was governed by (1) the availability of DEMs with appropriate (at least 30 m) horizontal resolution, and (2) the aim of including well-known examples with age constraint. Only Peléan domes and coulées were selected, having a range of compositional heterogeneity (from andesitic to rhyolitic).

The Ciomadul lava domes were analyzed using a 10 m-resolution DEM obtained by interpolation of contour line and spot elevations digitized from a 1:20,000 scale topographic map (with 10 m contour interval). Out of the five studied domes (Table 1), two have been assigned with radiometric ages (Fű-Haram, 136 ka, and Vár-tető, 127 ka, respectively), as average age estimates from (U–Th)/He dating (see Section 4.2).

A number of well-known lava domes have been included from the USA (Table 1), represented in the USGS NED DEM (Gesch et al., 2009) with 1/3″ (~10 m) or in some cases 1/9″ (~3 m) resolution. This data set is freely available at http://seamless.usgs.gov. Three domes have been selected from the High Cascades (the active Mt. St. Helens with the latest dome growth phase in 2008, the 1 ka old Chaos Crags at Mt. Lassen, and the 9.5 ka old Black Butte at Mt. Shasta); seven domes from the High Lava Plains in Oregon; and two domes from the Snake River Plain. The latter two fields comprise progressively older domes on the Ma scale, advantageous for understanding the relationship between morphometry and age.

In addition, 11 more domes including world-renowned examples have also been selected (Table 1). These include the above mentioned Puy-de-Dôme (last eruption 10,700 yr: Miailler et al., 2010), Mount Pelée (last eruption 1929), and Unzen (last eruption 1996). There are four more domes from Japan, three from the Valle de Bravo volcanic field, Mexico, one dome from Dominica, and one (M. Amiata) from Italy. M. Amiata is represented by the freely downloadable 10 m-resolution TINITALY data base (http://tinitaly.pi.ingv.it; Tarquini et al., 2007), whereas for the other domes we used the ASTER GDEM data set having 30 m horizontal resolution. As for the lower resolution of ASTER, previous studies (Kervyn et al., 2008; Grosse et al., 2012) proved that volcanic landforms of such dimensions (in the order of 1 km) are properly represented by the ASTER dataset. A further problem is that, at many locations, the ASTER dataset has not negligible vertical errors of some tens of meters (both noise and artifacts: see Huggel et al., 2008; Reuter et al., 2009); however, after the careful visual

Table 1
Geographical, geological, geochronological and morphometrical data of 29 lava domes from around the world with age constraints and the studied Ciomadul lava domes (in italics), arranged by lithology and within each class in alphabetic order.

Name	Latitude (°)	Longitude (°)	Age (ka)	$S_{R,1}$	$S_{R,2}$	$S_{S,1}$	$S_{S,2}$	$MeanS_1$	$MeanS_2$	$MaxS$	Lithology	Climate	Reference (including geochronology)
Microtin, Dominica, FR	15.341	−61.321	1.2	21.9	19.5	11.2	14.1	26.4	31.5	35.7	Andesite	VH	Volcano Hazard Report for Southern Dominica (2000)
M. Pelée, Martinique, FR	14.809	−61.166	0.08	40.1	26.1	35.8	25.8	34.0	34.5	36.7	Andesite	VH	Tanguy (2004)
Niigata, Honshu, J	36.921	138.036	0.65	25.2	20.2	23.1	18.7	26.8	30.7	36.2	Andesite–dacite	H	Global Volcanism Program[a]
M. Amiata, IT	42.890	11.626	300	22.5	12.2	19.8	14.8	20.9	20.7	24.5	Trachydacite	H	Ferrari et al. (1996)
Puy de Dome, FR	45.775	2.964	10.7	28.7	22.4	28.0	27.2	30.8	32.9	37.7	Trachyte	H	Miailler et al. (2010)
Atosanupuri (north), Hokkaido, J	43.629	144.418	1.3	35.8	21.8	39.0	23.8	35.5	32.7	41.6	Dacite	H	Global Volcanism Program[b]
Atosanupuri (middle), Hokk., J	43.615	144.427	1.3	18.2	18.5	30.5	21.6	22.5	28.4	35.8	Dacite	H	Global Volcanism Program[b]
Atosanupuri (south), Hokk., J	43.610	144.438	1.3	31.1	18.2	52.0	18.7	30.6	27.8	32.4	Dacite	H	Global Volcanism Program[b]
Bald, Or, USA	43.276	−121.357	5200	18.3	10.7	22.7	13.8	18.9	17.7	20.2	Rhyolite	A	Jordan et al. (2004)
Frederick, Or, USA	43.620	−120.465	4000	14.8	11.7	19.0	12.8	18.1	16.7	21.1	Dacite	A	Jordan et al. (2004)
Flores, MEX	19.423	−100.293	670	16.3	16.1	14.3	14.6	23.2	25.7	29.3	Dacite	A	Aguirre-Díaz et al. (2006)
Horsehead, Or, USA	43.166	−119.741	15600	12.5	n.d.	15.6	n.d.	13.4	12.2	17.1	Dacite	A	Jordan et al. (2004)
Jackass Butte, Or, USA	43.035	−118.943	15300	11.0	n.d.	14.8	n.d.	11.9	10.2	15.0	Dacite	A	Jordan et al. (2004)
Little Juniper, Or, USA	43.154	−119.846	15600	20.9	13.8	23.1	11.6	23.0	17.9	27.0	Dacite	A	Jordan et al. (2004)
St. Helens, Wa, USA	46.199	−122.190	0.004	24.0	21.6	42.1	22.8	31.1	34.1	39.2	Dacite	VH	Major et al. (2009)
Pachuca, MEX	19.433	−100.340	670	22.8	18.7	16.8	15.3	25.0	27.4	30.6	Dacite	A	Aguirre-Díaz et al. (2006)
Rincon Chico, MEX	19.170	−100.211	350	20.4	20.0	19.3	18.3	23.1	29.5	35.3	Dacite	A	Aguirre-Díaz et al. (2006)
Unzen, Kyushu, J	32.762	130.299	0.015	30.5	25.8	41.5	26.7	31.8	35.0	39.5	Dacite	H	Nakada et al. (1995)
Black Butte (Shasta), Or, USA	41.367	−122.349	9.5	30.7	25.0	37.5	27.6	37.1	36.0	42.4	Dacite	H	McCanta et al. (2007)
Chaos Crags (Lassen), Ca., USA	40.528	−121.520	1	31.2	20.5	28.6	20.9	34.2	34.3	36.9	Rhyolite	H	Christiansen et al. (2002)
China Hat, Or, USA	43.681	−121.034	780	21.1	11.8	21.1	12.9	21.2	18.8	23.2	Rhyolite	A	Jordan et al. (2004)
East Butte, Id, USA	43.497	−112.665	580	20.6	18.0	13.8	15.7	27.9	32.2	36.6	Rhyolite	A	McCurry et al. (1999)
East Butte, Or, USA	43.667	−120.996	850	19.5	12.9	21.8	14.0	19.1	20.1	21.4	Rhyolite	A	Jordan et al. (2004)
Middle Butte, Id, USA	43.490	−112.738	1000	18.5	16.7	17.9	15.9	21.7	25.9	31.7	Rhyolite	A	McCurry et al. (1999)
Haramul Ierbos (Fű-Haram)	*46.151*	*25.911*	*136*[c]	*26.5*	*19.5*	*28.1*	*19.5*	*24.2*	*25.1*	*27.5*	*Dacite*	*H*	*This study*
Vf. Cetății (Vár-tető)	*46.150*	*25.882*	*127*[c]	*38.4*	*24.7*	*46.7*	*30.4*	*32.5*	*32.0*	*35.7*	*Dacite*	*H*	*This study*
Vf. Comloș (Komlós-tető)	*46.137*	*25.876*		*22.6*	*23.1*	*38.4*	*25.0*	*22.4*	*26.3*	*35.8*	*Dacite*	*H*	*This study*
Haramul Mare (Nagy-Haram)	*46.157*	*25.915*		*24.7*	*19.4*	*27.2*	*18.8*	*27.3*	*28.6*	*30.0*	*Dacite*	*H*	*This study*
Vf. Surduc (Szurdok-tető)	*46.143*	*25.874*		*28.8*	*23.1*	*42.9*	*27.7*	*29.6*	*31.5*	*35.8*	*Dacite*	*H*	*This study*

S = slope. For definition of slope characteristics, see text.
VH = very humid (≥3000 mm), H = humid (≥800 mm) and A = arid (≤800 mm annual rainfall).
FR = France, J = Japan, IT = Italy, MEX = Mexico; Ca = California, Id = Idaho Or = Oregon and Wa = Washington.
[a] http://www.volcano.si.edu/world/volcano.cfm?vnum=0803-09=.
[b] http://www.volcano.si.edu/world/volcano.cfm?vnum=0805-08=&volpage=erupt.
[c] Averages of uncorrected age estimates from U–Th/He dating (see Fig. 5).

inspection of ASTER GDEM-derived contour maps and 3D images, it is concluded that the area of the selected lava domes are free of disturbing artifacts (except Microtin, Dominica).

As mentioned above, in order to find correlation between derived slope values and age, we have focused on selecting an appropriate section of the upper flank slope profile. During the calculation of representative upper flank slope values, most part of the surface area of each dome has been included. In the case of compound domes (i.e. those with a lobate shape), only the most regular dome shape was considered. Furthermore, some minor parts were excluded in the analysis of Microtin (Dominica) due to local ASTER GDEM errors.

When quantifying volcanic cone shapes based on DEMs, generalized profiles were used in several recent studies (e.g. Karátson et al., 2010a, 2010b, 2012; Grosse et al., 2012). The advantage of a generalized profile is that it is more representative than arbitrarily chosen single profiles or simple parameter values. Basically, two approaches can be applied in order to get a generalized profile. The first is when statistical parameters (min, max, mean, quartiles) of elevation (and slope) values are calculated and plotted as a function of radius (R, distance from cone center) as in Karátson et al. (2010a). The second approach is when statistics of different morphomeric parameters (e.g. slope, ellipticity, etc.) are calculated and plotted as a function of height, h (as in Wright et al., 2006; Karátson et al., 2010b; Grosse et al., 2012). In this study, we used the second approach, since lava domes are often less circular, truncated by erosion, or coalesced by other lava domes, issues that influence the results more significantly in case the first approach is used. The scheme of our calculation method is presented in Fig. 3. Height is calculated relative to the top of the lava dome (as zero). The novelty of our study is that R (distance from the cone center) is also calculated for a given height interval. The resultant R–h diagrams (Fig. 3 central panel) display the steepest, the mean and the gentlest descent from the top of the lava dome. The mean R–h curve is taken as the generalized profile of the dome. Apart from the R–h diagrams, we also calculated slope statistics (min, mean, max) at each height increment (Fig. 3 right).

It is obvious that the uppermost part of the lava domes is not representative for studying long-term changes due to the commonly broad summit with irregular topography. Therefore, we analyzed the slope sections starting below −50 m relative to the top elevation. We selected and calculated the following slope parameters:

$S_{R,1}$: The slope between −50 m and −100 m based on the mean R–h curve;

$S_{R,2}$: The slope between −50 m and −200 m based on the mean R–h curve;

$S_{S,1}$: The slope between −50 m and −100 m based on the minimum R–h curve (i.e. along the steepest descent);

$S_{S,2}$: The slope between −50 m and −200 m based on the minimum R–h curve;

$MeanS_1$: The mean slope between −50 m and −100 m based on the *Slope*–h curve (i.e. taking into account the real slope values, which are usually larger due to small-scale erosional landforms);

$MeanS_2$: The mean slope between −50 m and −200 m based on the *Slope*–h curve;

MaxS: The maximum slope between −50 m and −400 m (or lowermost height if the dome is smaller) based on the *Slope*–h curve.

Using these statistical parameters, correlations between different slope values and lava dome age have been determined.

As it can be seen in Table 1, lava dome ages span from recent to 15 Ma. Certainly, given such a long time interval, climate plays a major role in denudation processes and rates (e.g. Thouret, 1999). However, since it is not possible to quantify long-term climate data in detail, we did not add climatological constraints, but we indicated the type of the prevailing current climate: very humid (e.g. M. Pelée: 10,000 mm/yr, Mt. St. Helens: 5000 mm/yr rainfall), humid (e.g. Unzen: 3000 mm/yr, Ciomadul: 800 mm/yr rainfall), and arid (e.g. Oregon and Idaho domes with ~300 mm/yr rainfall). As exemplified by Fig. 4, the several Ma-old domes occur exclusively under arid climates, which imply low denudation rates and the resultant well-preserved landforms in these cases.

3.3. Morphometrical results

Comparing R–h curves and different slope values of lava domes, we obtained the following numerical results (Table 1). For the younger domes, the upper flank slope ($S_{R,1}$) is generally >30° according to the mean profiles. However, if the steepest descent is considered ($S_{S,1}$), the values are mostly >35°, exceeding in some cases 40° as well. The mean slopes ($MeanS_1$ and $MeanS_2$) are also above 30°, while the steepest 10 m-high intervals ($MaxS$) have >35° slopes. Therefore, 35–40° is a good estimate for the initial angle of the upper flank slopes. Apparently (as expected), there is no lithologic control on these values, i.e. there is no difference according to rock type.

In order to determine to what extent the different slope parameters used here are interchangeable, we analyzed the relationships of slope parameters in a correlation matrix (Table 2). It shows that slope factors calculated for a smaller (−50 to −100 m) height range are in good correlation with their pairs ($S_{R,1}$ with $S_{R,2}$; $S_{S,1}$ with $S_{S,2}$; $MeanS_1$ with $MeanS_2$) calculated over a larger (−50 to −200 m) height interval. The highest correlation is between the $MeanS$ parameters, probably due to the fact that the mean is a statistically robust parameter. Also,

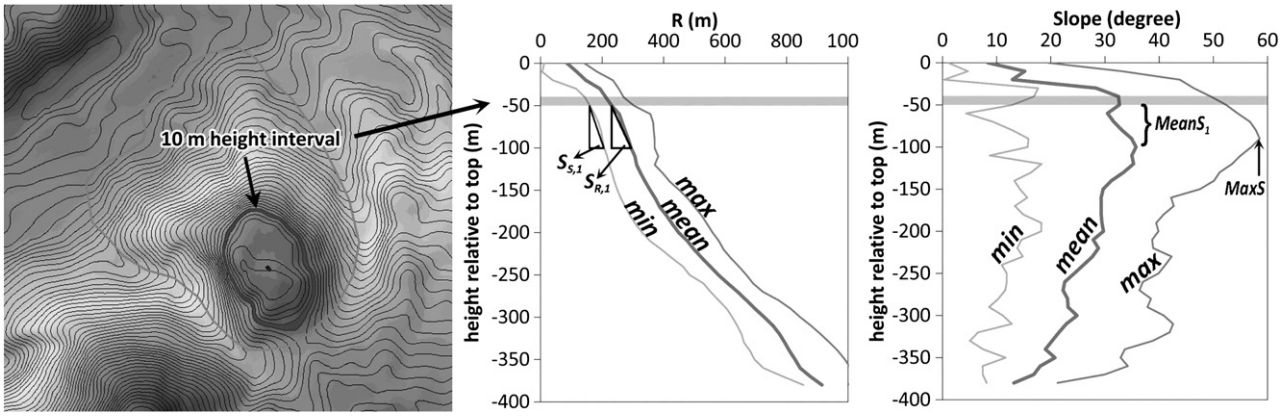

Fig. 3. Scheme of morphometrical calculations. Left: DEM of Vf. Cetății (Vár-tető) lava dome, with a selected 10 m height interval, the pixels of which are used to calculate gray stripes in the diagrams (the example is −50 m below summit); center: distance from dome center (R) vs. height diagram: the minimum, mean and maximum R–h curves correspond to the steepest, average and gentlest slope descent, respectively, along the flank; right: slope (S) vs. height diagram.

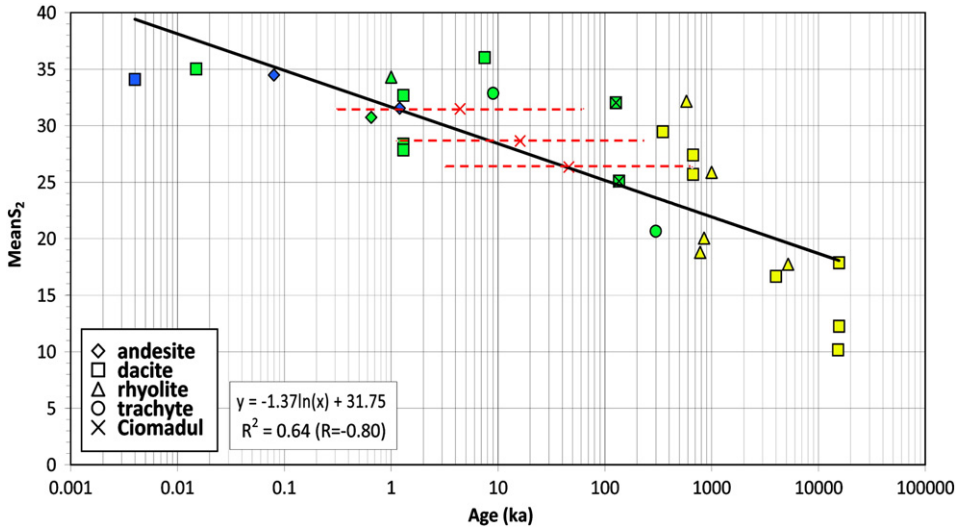

Fig. 4. Mean slope (S_2; °) vs age diagram. Blue (darker) color represents very humid, green color humid, and yellow (lighter) color arid climates. X symbols mark the Ciomadul (Csomád) lava domes and red X the calculated morphometric age for three domes without U age constraints, showing standard error bars (dotted line; see text). (For interpretation of the references to color in this figure legend, the reader is referred to the web version of this article.)

there are very good correlations between *MaxS* and other parameters (both $MeanS_1$ and $MeanS_2$ as well as $S_{R,2}$), which suggests that these are more or less interchangeable, i.e. any of them can typify the upper flank slope of lava domes. The most deviating parameters are $S_{S,1}$ and $S_{S,2}$ calculated on the basis of the steepest descent curve, implying that the steepest path is constrained by more specific factors controlling dome growth and erosion, and therefore is not interchangeable with other slope characteristics.

One of the most important questions is how slope changes with time. The highest correlations are obtained when logarithmic function is applied (Table 2, Fig. 4). Correlation coefficients (R) between the different slope parameters and the logarithm of age (Table 2) yield negative values from −0.64 and −0.80, which means that, indeed, there is a moderately strong inverse relationship between slope and age. The highest absolute correlation value of −0.80 proves that $MeanS_2$ reflects best the age-dependency.

Most Ciomadul lava domes have rather high slope values ($MeanS_2$ between 25° and 32°), although slightly lower than those of the youngest domes worldwide (e.g. 34–35° for Mt. St. Helens, Unzen, and M. Pelée). The logarithmic decrease in slope values implies that during the first intense erosion stage, subsequent to the formation of the lava domes, mass movements of weathered, loose material result in a rapid change in slope angle, whereas later on, the rate of change in slope angle gradually decreases with time (see Discussion).

Based on the equation in Fig. 4, an approximate "morphometric age" of lava domes can be calculated using backward regression if $MeanS_2$ is known. For the undated Ciomadul lava domes, we obtained very young age estimates: 50, 17 and 5 ka for Komlós-tető, Nagy-Haram and Szurdok-tető, respectively (standard error bars of estimated ages are indicated in Fig. 4). Mathematically, these young ages are implied from the steepness of most Ciomadul domes. Further implications and the likely reasons for these high slope angles (in addition to the young formation age) are discussed in Section 5.

Table 2
Linear correlation matrix (R values) of different slope parameters of lava domes.

Correlation matrix	$S_{R,1}$	$S_{R,2}$	$S_{S,1}$	$S_{S,2}$	$MeanS_1$	$MeanS_2$	*MaxS*
$S_{R,1}$	1.00	0.77	0.76	0.80	0.89	0.75	0.70
$S_{R,2}$	0.77	1.00	0.58	0.89	0.87	0.93	0.89
$S_{S,1}$	0.76	0.58	1.00	0.75	0.69	0.52	0.53
$S_{S,2}$	0.80	0.89	0.75	1.00	0.82	0.79	0.76
$MeanS_1$	0.89	0.87	0.69	0.82	1.00	0.92	0.91
$MeanS_2$	0.75	0.93	0.52	0.79	0.92	1.00	0.97
MaxS	0.70	0.89	0.53	0.76	0.91	0.97	1.00
Correlation with age	*−0.53*	*−0.45*	*−0.34*	*−0.45*	*−0.62*	*−0.75*	*−0.66*
Correlation with ln(age)	*−0.64*	*−0.73*	*−0.64*	*−0.64*	*−0.75*	*−0.80*	*−0.78*

4. Radiometric and paleoenvironmental constraints to the geochronological evolution

4.1. Assessment of available radiometric age data

The available K/Ar data on Ciomadul dome rocks show a high scatter ranging from 1 Ma to 220 ka (Table 3: Casta, 1980 Peltz et al., 1987 Pécskay et al., 1992, 1995; Szakács et al., 1993). In detail, the oldest dates come from the peripheral lava domes such as Kis-Haram and Cetatea Balvanyos (Bálványos), 850 ka and 1 020 ka, respectively (Casta, 1980; Pécskay et al., 1995; Fig. 1), whereas the coherent dome rocks of the inner volcanic structure (Nagy-Haram, 600 ka; Piscul Pietros [Köves Ponk], 560 ka) appear to be younger (Pécskay et al., 1992, 1995). Remarkably, Pécskay et al. (1992) published even younger, ~200 ka ages for lava dome rocks between Vf. Mohoş (Mohos-tető or Mohos-hegyese) and Fű-Haram. All these dates would suggest a very long (≤1 Ma) lava dome evolution, which seems unusual for such small complexes worldwide (e.g. ~280 ka at El Chichón: Espíndola et al., 2000; ~100 ka at M. Amiata: Ferrari et al., 1996).

The age of the explosive volcanic events is even more controversial. The pyroclastic series related to the earlier Mohos crater has not yet been dated. The pumiceous volcaniclastic deposit at Băile Tuşnad (Tusnádfürdő: Fig. 1), considered to represent one of the youngest eruptions of Ciomadul (see above), was dated at 42–35 ^{14}C ka BP (Moriya et al., 1995) and more recently at 43,250 ± 1000 cal yr BP (Harangi et al., 2010) by radiocarbon method on interbedded charcoal/charred wood fragments (Table 3). By contrast, biotite K/Ar dating (Pécskay et al., 1995) yielded much older ages of ~500 ka for the same deposit. However, K/Ar ages of few hundred thousand years old samples are frequently biased, especially when no pure K-bearing mineral fractions such as sanidine or leucite can be separated, and only whole rock or biotite phases are dated. Hora et al. (2010) have pointed that, in general, the dating of biotite often yields too old ages due to the presence of excess ^{40}Ar in the crystals. The youngest deposit at Ciomadul dated so far (31,450 ± 260 cal yr BP: Vinkler et al., 2007; Harangi et al., 2010: Fig. 1), also by the radiocarbon method on charcoal pieces, is a pumiceous block-and-ash flow deposit south of the Mohos crater.

Table 3
Published radiometric age data for the Ciomadul volcano.

Locality	Dated fraction	K/Ar ages (Ma, ka)	^{14}C ages		Reference
			^{14}C yr BP	Calibrated age (2σ) cal BP	
Cetatea Balvanyos (Bálványosvár)	Whole rock	1.0 ± 0.2			Pécskay et al. (1995)
	Whole rock	0.9 ± 0.2			Pécskay et al. (1995)
Haramul Mic (Kis-Haram)	Whole rock	0.85 ± ??			Casta (1980)
Haramul Mare (Nagy-Haram)	Whole rock	0.6 ± 0.2			Pécskay et al. (1995)
Piscul Pietros (Köves Ponk)	Biotite (from dacite lava)	0.56 ± 0.1			Pécskay et al. (1992)
Tusnad Bai (Tusnádfürdő), pumice quarry	Biotite (from dacite lapilli)	0.5 ± 0.0			Pécskay et al. (1995)
	Charcoal		10,700 ± 180	12,083–12,977	Juvigné et al. (1994)
	Charcoal		> 35,670		Moriya et al. (1996)
			> 35,520		
	Organic material in paleosoil		> 35,770		Moriya et al. (1995)
			> 42,650		
	Charcoal		38,700 ± 1000	41,673–44,530	Harangi et al. (2010)
	Humic acid		49,000 ± 3600		Harangi et al. (2010)
Vf. Mohos (Mohos-tető) N	Whole rock	221 ka ± 0.0			Pécskay et al. (1992)
		145 ka ± 0.0			
Bixad (Sepsibükszád) E	Charcoal		27,040 ± 450	30,741–32,437	Vinkler et al. (2007)
Bixad (Sepsibükszád) E	Charcoal		27,200 ± 260	31,095–31,887	Harangi et al. (2010)
	Humic acid		28,050 ± 290	31,514–33,068	Harangi et al. (2010)
	Charcoal		27,550 ± 270	31,245–32,510	Harangi et al. (2010)
	Humic acid		27,910 ± 270	31,454–32,892	Harangi et al. (2010)
St. Ana (Szent Anna) lake sediments in 17 m depth	Cladocera remains		21,685 ± 163	25,387–26,707	This study
Mohos peat bog	Peat moss		9750 ± 200	10,561–11,826	Tantau et al. (2003)

Whole rock = whole rock of coherent dacite lava.

The time constraints provided by the available radiometric data led to the generally accepted view on the twofold evolution of Ciomadul, involving a long-lasting lava-dome building stage followed by a short explosive phase (e.g. Szakács and Seghedi, 1996). However, the above assessment of the evolution of well-known lava dome complexes as well as the critical evaluation of K/Ar chronology render this hypothesis questionable.

4.2. U–Pb and (U–Th)/He geochronology

In order to better constrain the age of the volcanism, we performed zircon U–Pb and (U–Th)/He (ZHe) dating on samples from the northern and southern part of the lava dome complex at the rim of the craters, individual lava domes, as well as pumices from pyroclastic deposits (for sample location, see Fig. 1). The sampling strategy was to include both coherent lava dome and pyroclastic rocks as well as those already dated by either K–Ar or ^{14}C method. The U–Pb and (U–Th)/He geochronology has been performed in the Laboratory of University of Göttingen (for the description of the analytical procedure, see Löbens et al., 2011). Although this study is still in progress, the preliminary results can be used here to constrain the lifetime of the Ciomadul volcanic complex.

The U–Pb ages show a broad scatter and large variation even in individual samples. In Fig. 5, the age interval obtained from each location is presented. The single-crystal ages from the crater rims are ranging mostly between ~160 and 60 ka, while for the pumiceous deposit the variation is even larger, from ~180 to 40 ka. The scatter is significantly larger than the uncertainty of the individual ages. This spread of data could reflect the long-lasting pre-eruption evolution of the magma for a period of several hundred thousand years. Indeed, such a long residence time in the upper crustal magma chambers is often a phenomenon of silicic magmas (see e.g. Reid and Coath, 2000; Schmitt et al., 2003).

Compared to the U–Pb data, which usually record the pre-eruptive crystallization age, the age of the eruption can be constrained better by geochronometers having lower closure temperatures, like biotite or sanidine Ar/Ar or ZHe. Indeed, in some cases of the Ciomadul volcanic complex, the apparent ZHe ages are considerably younger than the U–Pb ages measured on the same deposit. We have to emphasize that the ZHe ages presented here are uncorrected minimum ages. They may be slightly younger than the true age of eruption, because at the current stage of measurements we could not perform the required disequilibrium corrections for the U-decay chain (Farley et al., 2002; Danišík et al., 2012).

Remarkably, the ZHe ages of samples collected from lava domes along the northern and southern rim of the craters differ significantly (Fig. 5). The (U–Th)/He ages of zircon crystals in a sample collected at the northern crater rim (Ciomadul Mic [Kis-Csomád] and Mohos-tető: Fig. 1) is similar to the U–Pb ages measured in the same sample (~100 ka), whereas the lava dome sample from the southern rim (Köves Ponk) yielded apparent ZHe ages around 40 ka. This indicates that the northern crater rim is composed of rocks generated by older eruptive activity compared to the rocks of the southern rim. Two peripheral lava domes (Vár-tető and Fű-Haram) appear roughly coeval with the northern crater domes having > 100 ka ages with relatively small scatter.

The zircon samples from the pumiceous-fall and -flow deposits, that were considered to represent the youngest explosive phase by ^{14}C dating, yielded apparent ZHe ages around 40 ka. The statistical tests for normality indicate that the age population is homogeneous if the youngest and oldest ages are rejected. Thus we can conclude that the pumice samples derived from the explosive volcaniclastic rocks are significantly younger than the lava domes of the northern crater rims and, possibly, they are coeval with the Köves-Ponk lava dome at the southern crater rim of Mohos.

4.3. Additional evidence from the sedimentary deposits of St. Ana (Szent Anna) lake

Currently, lake St. Ana is about 6 m deep but there is geomorphological evidence in the form of raised shorelines suggesting that the lake depth exceeded 12 m in the past (Gelei, 1909; Bányai, 1940; Pál, 2001). The sedimentary record of this lake has been studied intensely during the past decade following the recovery of a 4-m long sediment core (SZA-2001) that consisted mainly of fine gyttja (Magyari et al., 2006, 2009). The basal part of this core was dated at 8050 ± 50 ^{14}C yr BP (Table 4), however, since radiocarbon dating suggested older age for the last eruption(s) at or near St. Ana crater (see above), a new, 12 m-long sediment core (11 m undisturbed piston core + 1 m spiral core) was recovered in 2010.

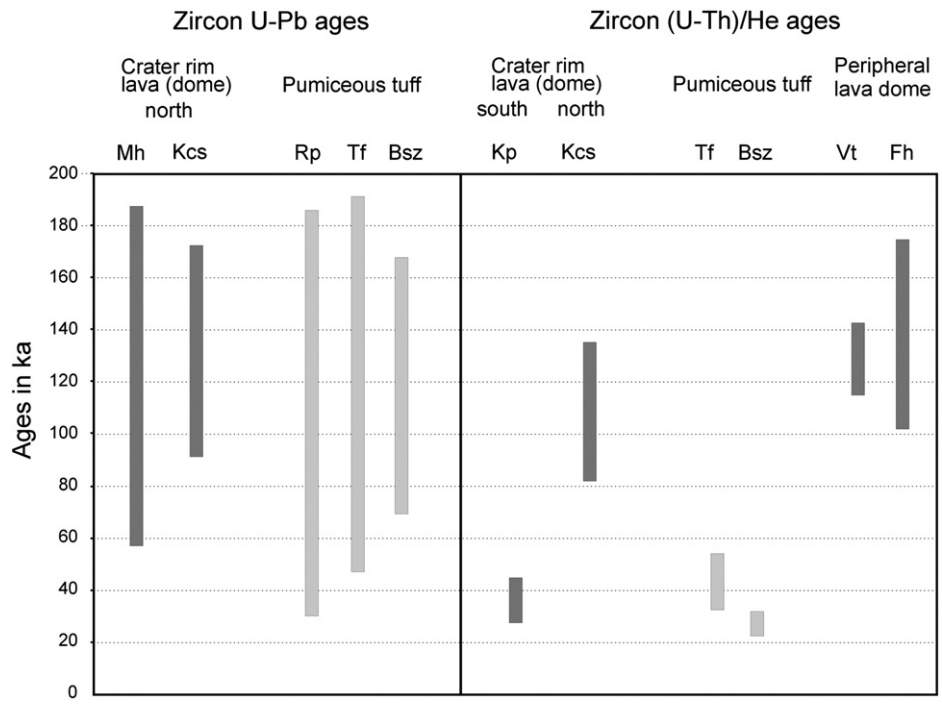

Fig. 5. Range of obtained single crystal U–Pb and (U–Th)/He ages of zircons in selected samples (for locality, see Fig. 1). Abbreviations: Mh = Vf. Mohoş (Mohos-tető), Kcs = Ciomadul Mic (Kis-Csomád), Rp = Románpuszta, Tf = Băile Tuşnad (Tusnádfürdő) quarry, Kp = Piscul Pietros (Köves-Ponk), Bsz = Bixad (Sepsibükszád) road cut, Vt = Vf. Cetăţii (Vár-tető) and Fh = Haramul Ierbos (Fű-Haram). The ZHe ages are corrected for alpha-ejection (according to Farley et al., 1996), but uncorrected for possible effect of the U-series disequilibrium. Three U–Pb ages older than 200 ka were measured mainly in the inherited cores of the crystals and therefore they are not presented on the plot.

Apart from the Holocene gyttjas, the sediment record consists mainly of highly minerogenic clayey silts typical of lacustrine sedimentation under stadial conditions (Veres et al., 2008). Fig. 6 shows the organic matter contents of sediment cores SZA-2001 (SZA-AB-3) and SZA-2010 together with the available magnetic susceptibility (MS) and fossil pollen data. The stratigraphic position of the previous and newly obtained radiocarbon age constraints is also shown. Dating of the organic-poor glacial part of the sediment was difficult as terrestrial plant macrofossils were largely absent from this sediment section and total organic content is below 5%. The lowermost available radiocarbon sample comes from the near-bottom part of the SZA-2010 piston core and provides an age of 26,050 ± 660 cal yr BP at 1682 cm core depth (1082 cm sediment depth). The carbon content of this sample was only 0.09 mg, but the applied extended counting time has been shown to provide reliable AMS ^{14}C readings in several cases (Santos et al., 2007). Further radiocarbon dates above this level decrease consistently with core depth supporting that the core–bottom minimum age is a reliable age estimate (Fig. 6). To support the evidence from radiocarbon dating of the SZA-2010 core, we considered information from other proxies as well.

The organic matter variations reflect productivity changes and point to considerably increased catchment and in-lake organic productivity during the Holocene above 1040 cm depth. The onset of the late glacial warming (Greenland Interstadial (GI)-1 at 14,500 cal yr BP) can be placed at 1070 cm on the basis of the increase of pine pollen percentages (Sum *Pinus*) and organic matter, and decreasing MS values. Below 1070 cm several intervals with well-expressed susceptibility increases reflect the input of detrital inorganic material likely associated with increased erosion and/or dust deposition under full glacial conditions. Magnetic susceptibility variations are often interpreted as reflecting cooling and warming events in lacustrine records (Veres et al., 2008) covering MIS 2 and 3 (14,500–60,000 cal yr BP), and the pattern observed in our data hints at the millennial-scale climate fluctuations specific of these periods (Dansgaard et al., 1993). Thus, increased erosion during cold phases (stadials) is usually associated with high susceptibility readings due to higher input of minerogenic materials (including magnetic minerals) into the lake basin, and limited dilution by in-lake organic productivity (Veres et al., 2008, 2009). Heinrich-events, i.e. extreme cold conditions coincident with releases of sea ice and icebergs into the North Atlantic from the neighboring ice sheets,

Table 4
Results of the AMS ^{14}C measurements from core SZA-AB3 (Magyari et al., 2009) and SZA-2010 (this paper) of Lake Sf. Ana. Conventional ages were calibrated with Calib 6.1.0. (Stuiver and Reimer, 1993; Calibration curve: IntCal09, Reimer et al., 2009). No correction for reservoir effects was performed.

Laboratory code	Dated material	Core	Depth below water surface (cm)	^{14}C ages BP	Calibrated BP age ranges (2σ)	Mid-point of 2σ calibrated age range
Poz-16074	*Fagus* sylvatica budscale	SZA-AB3	620–625	885 ± 30	732–833	782
Poz-9981	*Fagus* sylvatica budscale, leaf fragments	SZA-AB3	720–725	1185 ± 30	1051–1179	1115
Poz-9980	*Fagus* sp. budscale, leaf fragments	SZA-AB3	870–874	2970 ± 35	3004–3261	3132
Poz-9979	*Picea abies* seed	SZA-AB3	908–910	3475 ± 30	3685–3835	3760
Poz-9978	*Picea abies* seed	SZA-AB3	958–960	4830 ± 40	5473–5552	5512
Poz-16075	*Betula pubescens* seed	SZA-AB3	988–990	7170 ± 50	7927–8061	7994
Poz-9976	*Acer* seed	SZA-AB3	1012–1014	8050 ± 50	8725–9039	8882
COL1123.1.	Cladocera eggs and Chironomid head capsules	SZA-2010	1339–1342	17,340 ± 85	20,290–21,138	20,715
COL1127.1.	moss leaves, Cladocera eggs and Chironomid head capsules	SZA-2010	1538–1540	19,720 ± 120	23,133–23,953	23,545
COL1128.1.1	Chironomid and Cladocera remains, particular organic matter	SZA-2010	1682	21,685 ± 163	25,387–26,707	26,047

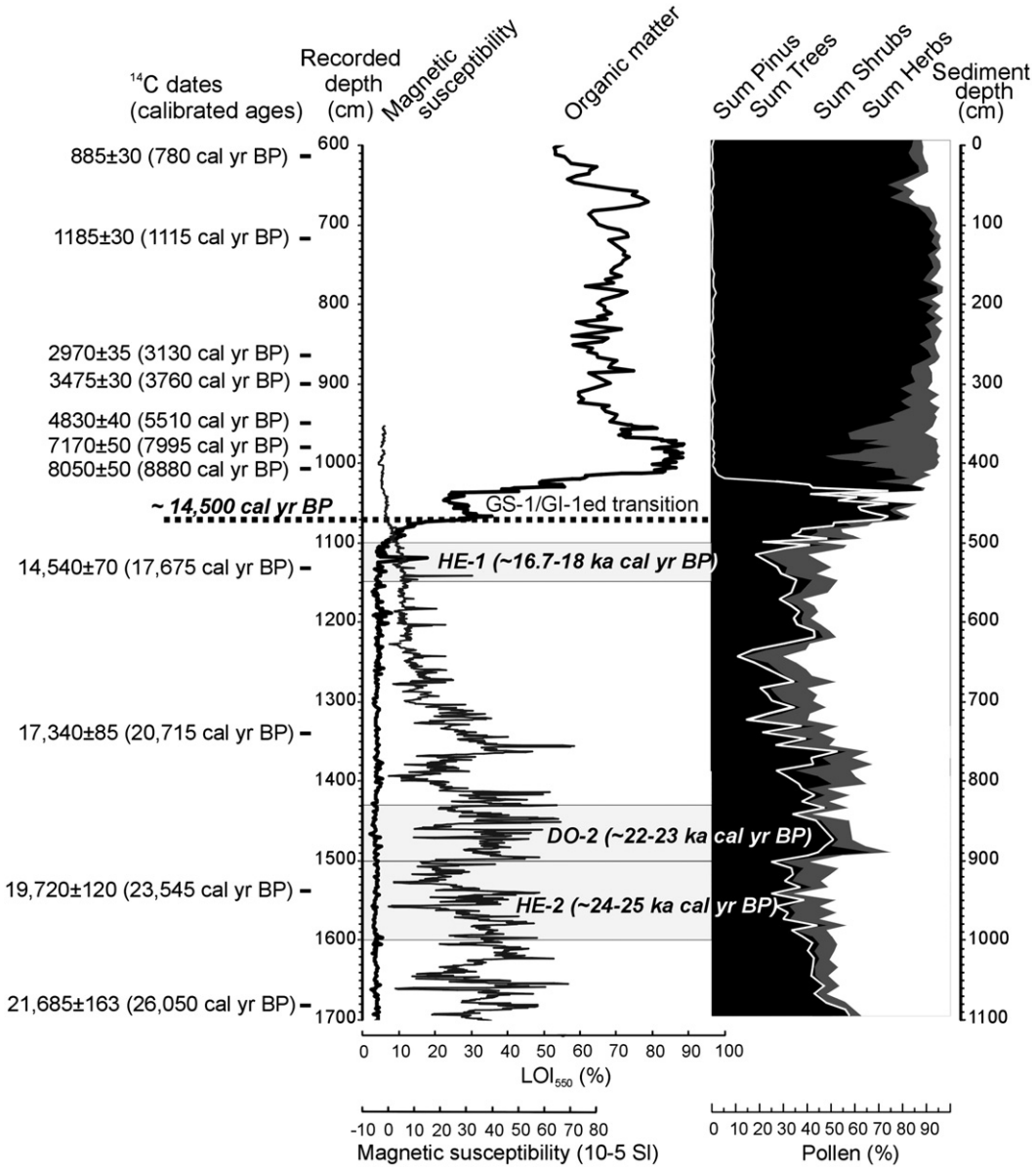

Fig. 6. AMS ^{14}C dates, magnetic susceptibility and preliminary pollen results from the combined SZA-AB3 and SZA-2010 sediment records, Lake Sf. Ana (Szent Anna), Romania. LOI_{550}: loss-on-ignition at 500 °C; H-1: Heinrich event 1 and DO-2: Dangaard-Oeschger interstadial 2.

occurred during some, but not all, of the periodic cold spells preceding the rapid warming GI events (Hemming, 2004). Although very tentatively, the MS peaks in the SZA-2010 record may reflect the impact of these cold spells, and several such large variations can be observed in the susceptibility record (Fig. 6). Using the age estimates of Hemming (2004) for the timing of Heinrich-events, we infer that the SZA-2010 core clearly extends beyond HE-1 (16,800 cal yr BP) and certainly covers HE-2 (24,000 cal yr BP). Pollen composition of the bottom-most recovered sediment sample (1185 cm sediment depth) suggests that at the time of sediment deposition the regional vegetation consisted of mixed-leaved boreal forest and cold continental steppe. Notable is the relatively high percentage of deciduous trees (*Betula*, *Ulmus*, *Fraxinus*, *Corylus*, *Carpinus betulus*, *Fagus*) and *Pinus* (Table 5), typical of interstadial conditions.

Overall, the paleolimnological data suggest that the sedimentary basin formed in the St. Ana crater supported lacustrine sedimentation by at least 26,000 cal yr BP based on the radiocarbon data, but very likely earlier considering information from pollen data. Given that no volcanic breccia or other large pyroclastic fragments were observed in the sediment core, it is likely that the bottom of the lake sediment infill has not yet been reached.

5. Discussion

5.1. Lava dome morphometry and chronology

Results of the morphometric analysis of Ciomadul lava domes, compared to a number of well-known domes worldwide, unambiguously suggest a very young age for the lava dome volcanism in the study area. However, at first, the landform evolutionary meaning of data presented in Fig. 4 with regard to both short- and long-term erosion should be discussed.

As shown for several volcano types such as scoria cones or stratovolcanoes, initial rapid erosion slows down in some tens of thousands of years due to (a) the consolidation of loose tephra and/or removal of fragmented material (e.g. lava flow surfaces, debris flows), and (b) afforestation (Ollier, 1988; Karátson, 1996; Favalli et al., 2009; Karátson et al., 2012). According to Fig. 4, this rule is valid for lava

Table 5
Relative pollen abundances of the most important pollen types at 1785 cm core length in Lake Sf. Ana. Sample was taken by a spiral corer in 2010 to test sediment availability and composition. Below 1700 cm the undisturbed piston core (SZA-2010) terminated due to technical problems.

Sum *Pinus*	40.7%
Betula	7.4%
Ulmus	5.4%
Fraxinus	2.0%
Corylus	1.4%
Fagus	2.0%
Carpinus betulus	1.4%
Other trees & shrub pollens	8.3%
Poaceae	11.7%
Artemisia	8.1%
Chenopodiaceae	1.8%
Other herb pollens	9.9%

domes as well, supported by the fact that the correlation between slope and the logarithm of age is significantly better than the linear correlation between slope and age. Whereas steep, linear upper flank slopes are primary features reflecting constructive dome-building processes and yield strength of lava, we suggest that the gentler and/or concave lower slopes are secondary features, resulting from progressive erosion (e.g. downhill redeposition of upper slope material; cf. Thouret, 1999). The reason is that, during the degradation of lava domes, fragmented dome rock as well as slope debris are transported and accumulated downslope, producing more gentle slopes.

On the other hand, the inferred gradually decreasing change in slope with time cannot be applied as a simple rule, because it depends also on climatic conditions. Although we could not quantify long-term paleoclimate data including major climate changes, it is obvious that any significant climate change modifies long-term erosion rates, causing uncertainties when inferring "morphometric ages". Short-term erosion rates on the hundred thousand year order may also show big differences due e.g. to variations in precipitation (amount and intensity) and temperature as well as afforestation. Besides initial shape deviations, differential erosion may be the factor behind the reason that, in fact, we have found many young (1–10 ka old) domes showing relatively large differences in mean slope (27–36°).

However, at Ciomadul, apart from the effect of moderately humid mountain climate that prevailed during the current interglacial (Magyari et al., 2009), there may be at least two more additional factors enhancing erosion. Some of the domes, especially Szurdok- and Komlós-tető, are facing the Tusnád Gorge. The ongoing downcut of river Olt since the Late Pleistocene (Section 5.2) has accelerated the erosive power on the hillslopes; as a result, slope angles could be higher relative to their age, thus their morphometric age might underestimate the real ages. In addition, in the case of the above domes as well as Vár-tető, the asymmetric emplacement (i.e. coulee) could have also increased the slope values.

Taking these considerations into account, we consider the obtained morphometric ages (50–5 ka) as minimum estimates. However, there is no question that these ages do not conform with the several ka old K/Ar ages (for example the 17 ka morphometric age of Nagy-Haram opposed to its 0.6 Ma K/Ar age).

At the same time, the results from zircon dating largely confirm the scenario outlined by the DEM analysis. When evaluating zircon ages, it should be noted first that without U-series disequilibria corrections the (U–Th)/He zircon ages often underestimate the eruption age, due to the disequilibria in zircon (Farley et al., 2002). Nevertheless, it is noteworthy that very similar ages were obtained by radiocarbon dating (e.g. Harangi et al., 2010) and average estimates from (U–Th)/He dating for two localities (~30 ka for a block-and-ash flow deposit outcrop close to Bixad and ~42 ka for the pumice quarry near Băile Tuşnad: Fig. 1).

Although determining the precise age of individual lava domes and explosive eruptions needs further radiometric studies, our twofold approach unequivocally suggests that the volcanic activity in the area is much younger than previously determined (e.g. Pécskay et al., 1995): the morphometric analysis yields ages <100 ka, whereas the presented zircon dating implies eruption ages <200 ka. Furthermore, we infer that no clear distinction between an effusive and a subsequent explosive phase existed, in consistence with the general eruptive behavior of dacitic lava dome complexes worldwide (e.g. Fink and Anderson, 2000).

5.2. Summary of the volcanic evolution, and paleogeographic implications

The volcanic activity of the Ciomadul lava dome complex over the past ~200–250 ka has been typical of andesitic–dacitic lava domes, producing coeval effusive and explosive (i.e. vulcanian) eruptions. Pyroclastic sequence in low stratigraphic position at Mohos, and late-stage pumiceous pyroclastics likely related to the formation of St. Ana crater, point to periodically more violent explosive eruptions, that may have occurred during the entire growth of the lava dome complex. Given this occasional highly explosive activity, and considering the typical, successive crater-forming events at other well-studied lava dome complexes worldwide (e.g. El Chichón, Mexico; Soufrière Hills, Montserrat; Pululagua, Ecuador), we propose that the central morphology of Ciomadul is not as simple as previously thought (i.e. a simple twin-cratered edifice). It is more likely that during its history several crater- and nested crater-forming eruptions may have occurred. As a remnant of these, the flat, uniform, higher northern lava-dome rim encompassing the present-day craters (described in Section 2.1) may represent a larger explosion crater (2–2.5 km in diameter: Figs. 1, 2 and 7); the present-day craters could be just the very final landforms cutting previous structures. Such a hypothesis, obviously, should be supported by identifying the related deposits from highly explosive eruptions, which will be the task of further detailed mapping. We note the geomorphic similarity of the suggested large crater rim to that of Mt. Somma, as already mentioned by Bányai (1940).

The young age of the whole volcanism obtained in our study brings important paleogeographical implications. In case the ages of the third and fourth river terraces of the river Olt are younger than ≤130 ka (see Section 2.1), they could be slightly younger that the beginning of volcanic activity (according to our zircon dating). In such a scenario, an epigenetic origin of the Olt valley can be inferred, i.e. the river valley may have appeared subsequently relative to the onset of volcanism at Ciomadul. Such an age relation supports the concept of Bulla (1948), who however suggested "early Pleistocene" oldest terraces and even older age for the volcanic activity.

The timing of the very last eruption of the St. Ana crater can be constrained indirectly through the coring and dating of its deposits. The available evidence suggests that at least for the last 26 ka BP the Sf. Ana crater underwent continuous lacustrine sedimentation. This age estimate is somewhat younger than the proposed latest radiocarbon-dated eruption of Ciomadul (31,450 yr BP: Harangi et al., 2010). However, the coring has not yet reached the crater bottom and, on the other hand, the latter age may not necessarily reflect eruptive activity from the main crater; more likely, it could be related to a roughly coeval satellite dome activity as suggested by (U–Th)/He dating. More importantly for a better understanding of the current volcanic geomorphology, it should be stressed that the volcanic activity at St. Ana, the youngest crater of the whole Carpathians, ceased ≥26 ka ago. It will be the subject of further studies whether the volcanism went extinct or is just undergoing a dormancy phase.

6. Conclusions

1. The Ciomadul (Csomád) volcano is a common type of andesitic–dacitic lava dome complex similar to such volcanoes worldwide that underwent alternate effusive and explosive activities throughout

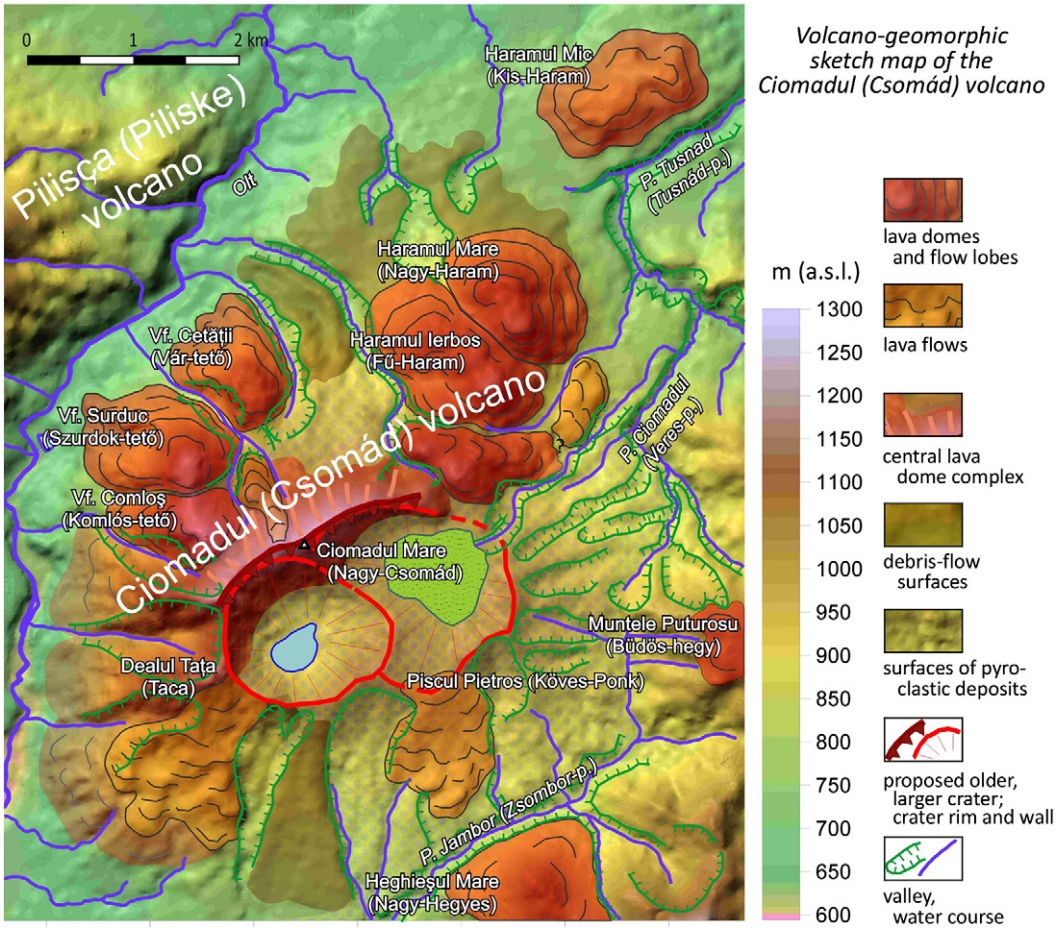

Fig. 7. Volcano-geomorphic sketch map of the Ciomadul (Csomád) volcano, on the basis of Szakács and Seghedi (1986, 1990), Moriya et al. (1995), and own field data.

their history. At Ciomadul, the explosive phases included more explosive e.g. subplinian eruptions as well, producing widespread tephra.

2. Peléan domes and asymmetric domes/coulées are the most typical landforms at Ciomadul (Fig. 7), whose ages have been constrained by comparative morphometry and radiometric chronology. DEM-based morphometric analysis suggests ≤100 ka minimum ages for the studied domes. These ages are roughly matched by results of the present stage of zircon dating by the U/Pb and (U–Th)/He methods constraining the volcanic activity between ~200/250–30 ka and the emplacement of most lava domes ~150–100 ka.
3. As for the evolution of the dome complex, a central edifice may have formed partly coevally with the peripheral domes. The available volcanological and geomorphological data, in accordance with worldwide analogies, point to a successive evolution of smaller and larger central craters. The last highly explosive eruptions may have formed the Mohos and subsequently the youngest St. Ana crater. Whereas the eruptive history of the Mohos crater, completely infilled by a thick volcanic-sedimentary succession overlain by 10 m-thick peat deposit, has not yet been constrained, the age model for the top ~11 m lacustrine infill of Lake St. Ana implies that this younger crater already existed prior to 26 ka BP.

Acknowledgments

The research activities were funded by Hungarian National Research Funds T68587 and NF101362. D. V. acknowledges the support of SOPHRD 2007–2013 under the project no./POSDRU/89/1.5/S/60189. This is MTA-MTM contribution No. 174. We thank Ioan Seghedi for his constructive remarks on the earlier draft of the manuscript, and two anonymous reviewers for their helpful comments.

References

Aguirre-Díaz, G.J., del Carmen Jaimes Viera, M., Nieto-Obregón, J., 2006. The Valle del Bravo Volcanic Field: geology and geomorphometric parameters of a Quaternary monogenetic field at the front of the Mexican Belt. In: Siebe, C., Macías, J.L., Aguirre-Díaz, G.J. (Eds.), Neogene-Quaternary Continental Margin Volcanism: A Perspective from México: Geol. Soc. Amer. Spec. Pap., 402.

Anderson, S.W., Fink, J.H., Rose, W.I., 1995. Mount St. Helens and Santiaguito lava domes: the effect of short-term eruption rate on surface texture and degssing processes. Journal of Volcanology and Geothermal Research 69, 105–116.

Bányai, J., 1940. A Szent Anna tó és környéke (Lake St. Ana and its surroundings). Attachment to the Periodical "Székelység".Jadál Gábor könyvnyomdája, Ordorheiu Secuiesc (Székelyudvarhely).

Blake, S., 1990. Viscoplastic models of lava domes. In: Fink, J.H. (Ed.), Lava Flows and Domes: Emplacement Mechanisms and Hazard Implications. Springer, New York, pp. 88–126.

Boccaletti, M., Manetti, P., Peccerillo, A., Peltz, S., 1973. Young volcanism in the Calimani–Harghita Mountains (East Carpathians): evidence of paleoseismic zone. Tectonophysics 19, 299–313.

Bulla, B., 1948. A két Csiki-medence és az Olt-völgy kialakulásáról (On the formation of the two Ciuc Basins and Olt valley). Földrajzi Közlemények (Bull. Hung. Geogr. Soc.), Budapest, LXXVI, pp. 134–156. in Hungarian.

Casta, L., 1980. Les formation quaternaires de la depression de Brasov (Roumaine). PhD Thesis, Université d'Aix Marseille II.

Cholnoky, J., 1922. Néhány vonás az Erdélyi-medence földrajzi képéhez. III. Hargita (Contributions to the Geography of Transylvanian Basin. III. Harghita Mts.) : Földrajzi Közlemények (Bull. Hung. Geogr. Soc.), Budapest, 50, 2, pp. 107–122. in Hungarian.

Cholnoky, J., 1943. Erdélyi képek (Pictures from Transylvania). in Hungarian Franklin Társulat, Budapest (164 pp.).

Christiansen, R.L., Clynne, M.A., et al., 2002. Geologic map of the Lassen Peak, Chaos Crags, and Upper Hat Creek area, California: US Geol. Surv. Geologic Investigations Series, I-2723.

Danišík, M., Shane, P.A.R., Schmitt, A.K., Hogg, A., Santos, G.M., Storm, S., Evans, N.J., et al., 2012. Re-anchoring the late Pleistocene tephrochronology of New Zealand

based on concordant radiocarbon ages and combined $^{238}U/^{230}Th$ disequilibrium and (U–Th)/He zircon ages. Earth and Planetary Science Letters 349–350, 240–250.
Dansgaard, W., Johnsen, S.J., Clausen, H.B., Dahl-Jensen, D., Gundestrup, N.S., Hammer, C.U., Hvidberg, C.S., Steffensen, J.P., Sveinbjoernsdottir, A.E., Jouzel, J., 1993. Evidence for general instability of past climate from a 250-kyr ice-core record. Nature 364 (6434), 218–220.
de Silva, S., Self, P., Francis, P.W., Drake, R.E., Ramirez, R.C., 1994. Effusive silicic volcanism in the Central Andes: the Chao dacite and other young lavas of the Altiplano-Puna Volcanic Complex. Journal of Geophysical Research 99 (B9), 17,805–17,825.
Espíndola, J.M., Macías, J.L., Tilling, R.I., Sheridan, M.F., 2000. Volcanic history of El Chichón Volcano (Chiapas, Mexico) during the Holocene, and its impact on human activity. Bulletin of Volcanology 62, 90–104.
Farley, K.A., Wolf, R., Silver, L., 1996. The effects of long alpha-stopping distances on (U–Th)/He ages. Geochimica et Cosmochimica Acta 60, 4223–4229.
Farley, K.A., Kohn, B.P., Pillans, B., 2002. The effects of secular disequilibrium on (U–Th)/He systematics and dating of Quaternary volcanic zircon and apatite. Earth and Planetary Science Letters 201, 117–125.
Favalli, M., Karátson, D., Mazzarini, F., Pareschi, M.T., Boschi, E., 2009. Morphometry of scoria cones located on a volcano flank: a case study from Mt. Etna volcano (Italy), based on high-resolution LiDAR data. Journal of Volcanology and Geothermal Research 186, 320–330. http://dx.doi.org/10.1016/j.jvolgeores.2009.07.011.
Ferrari, L., Conticelli, S., Burlamacchi, L., Manetti, P., 1996. Volcanological evolution of the Monte Amiata, Southern Tuscany: new geological and petrochemical data. Acta Vulcanologica 8, 41–56.
Fielitz, W., Seghedi, I., 2005. Late Miocene-Quaternary volcanism, tectonics and drainage system evolution on the East Carpathians, Romania. In: Cloetingh, S., et al. (Ed.), Special Volume Fourth Stephan Müller Conference of the EGU on Geodynamic and Tectonic Evolution of the Carpathian Arc and its Foreland: Tectonophysics, 410, pp. 111–136.
Fink, J.H., Anderson, S.W., 2000. Lava domes and Coulees. In: Sigurdsson, et al. (Ed.), Encyclopedia of Volcanoes. Academic Press, pp. 307–319.
Fink, J.H., Bridges, N.T., 1995. Effects of eruption history and cooling rate on lava dome growth. Bulletin of Volcanology 57 (4), 229–239.
Fink, J.H., Griffiths, R.W., 1998. Morphology, eruption rates, and rheology of lava domes: insights from laboratory models. Journal of Geophysical Research 103, 527–545.
Fornaciai, A., Favalli, M., Karátson, D., Tarquini, S., Boschi, E., 2012. Morphometry of scoria cones, and their relation to geodynamic setting: a DEM-based analysis. Journal of Volcanology and Geothermal Research 157–158, 56–72. http://dx.doi.org/10.1016/j.jvolgeores.2011.12.012.
Gelei, J., 1909. A Szent Anna-tó (Lake Sf. Ana). Földrajzi Közlemények (Bull. Hung. Geogr. Soc.), Budapest, 47, pp. 177–201. in Hungarian.
Gesch, D., Evans, G., Mauck, J., Hutchinson, J., Carswell Jr., W.J., 2009. The national map—elevation. U.S. Geological Survey Fact Sheet 2009–3053 (4 pp.).
Grosse, P., van Wyk de Vries, B., Euillades, P.A., Kervyn, M., Petrinovic, I.A., 2012. Systematic morphometric characterization of volcanic edifices using digital elevation models. Geomorphology 136 (1), 114–131.
Hale, A.J., Wadge, G., 2008. The transition from endogenous to exogenous growth of lava domes with the development of shear bands. Journal of Volcanology and Geothermal Research 171, 237–257.
Harangi, S., Lenkey, L., 2007. Genesis of the Neogene to Quaternary volcanism in the Carpathian–Pannonian region: role of subduction, extension, and mantle plume. Geological Society of America Special Papers 418, 67–92.
Harangi, Sz, Molnár, M., Vinkler, A.P., Kiss, B., Jull, A.J.T., Leonard, A.E., 2010. Radiocarbon dating of the last volcanic eruptions of Ciomadul volcano, Southeast Carpathians, eastern–central Europe. Radiocarbon 52 (2–3), 1498–1507.
Hemming, S.R., 2004. Heinrich events: massive late Pleistocene detritus layers of the North Atlantic and their global climate imprint. Reviews of Geophysics 42, RG1005. http://dx.doi.org/10.1029/2003RG000128.
Hora, J.M., Singer, B.B., Wörner, G., 2010. Volcano evolution and eruptive flux on the thick crust of the Andean Central Volcanic Zone: $^{40}Ar/^{39}Ar$ constraints from Volcán Parinacota, Chile. Geological Society of America Bulletin 119 (3–4), 343–362. http://dx.doi.org/10.1130/B25954.1.
Huggel, C., Schneider, D., Julio Miranda, P., Delgado Granados, H., Kääb, A., 2008. Evaluation of ASTER and SRTM DEM data for lahar modeling: a case study on lahars from Popocatépetl Volcano, Mexico. Journal of Volcanology and Geothermal Research 170, 99–110.
Jordan, B.T., Grunder, A.L., Duncan, R.A., Deino, A.L., 2004. Geochronology of age-progressive volcanism of the Oregon High Lava Plains: implications for the plume interpretation of Yellowstone. Journal of Geophysical Research 109, B10202. http://dx.doi.org/10.1029/2003JB002776.
Juvigné, E., Gewelt, M., Gilot, E., Hurtgen, C., Seghedi, I., Szakács, A., Gábris, Gy., Hadnagy, Á., Horváth, E., 1994. Une éruption vieille d'environ 10 700 ans (^{14}C) dans les Carpates orientales (Roumanie). Comptes Rendus de l'Académie des Sciences, 318, pp. 1233–1238 (ser. II, Paris).
Karátson, D., 1994. A Hargita és a Görgényi-havasok vulkánossága, elsődleges formakincse és mai felszínének kialakulása (Volcanism of Harghita and Gurghiu Mts., their primary landforms, and formation of the present relief). Földrajzi Közlemények (Bull. Hung. Geogr. Soc.), Budapest, CXVIII (XLII), pp. 83–111. in Hungarian with English abstract.
Karátson, D., 1996. Rates and factors of stratovolcano degradation in a continental climate: a complex morphometric analysis of nineteen Neogene/Quaternary crater remnants in the Carpathians. Journal of Volcanology and Geothermal Research 73, 65–78.
Karátson, D., 2007. A Börzsönytől a Hargitáig — vulkanológia, felszínfejlődés, ősföldrajz. (From Börzsöny To Harghita Mts. — Volcanology, Surface Evolution, Paleogeography). Typotex Kiadó, Budapest. ISBN: 978-963-9664-66-1. In Hungarian (463 pp.).
Karátson, D., Timár, G., 2005. Comparative volumetric calculations of two segments of the Neogene/Quaternary volcanic chain using SRTM elevation data: implications for erosion and magma output rates. Zeitschrift fur Geomorphologie Supplementband 140, 19–35.
Karátson, D., Telbisz, T., Singer, B.B., 2010a. Late-stage volcano-geomorphic evolution of the Pleistocene San Francisco Mountain, Arizona (USA), on the basis of high-resolution DEM analysis and Ar–Ar chronology. Bulletin of Volcanology 72, 833–846. http://dx.doi.org/10.1007/s00445-010-0365-8.
Karátson, D., Favalli, M., Tarquini, S., Fornaciai, A., Wörner, G., 2010b. The regular shape of stratovolcanoes: a DEM-based morphometrical approach. Journal of Volcanology and Geothermal Research 193, 171–181. http://dx.doi.org/10.1016/j.jvolgeores.2010.03.012.
Karátson, D., Telbisz, T., Wörner, G., 2012. Erosion rates and erosion patterns of Neogene to Quaternary stratovolcanoes in the Western Cordillera of the Central Andes: an SRTM DEM based analysis. Geomorphology 139–140, 122–135. http://dx.doi.org/10.1016/j.geomorph.2011.10.010.
Kervyn, M., Ernst, G.G.J., Goossens, R., Jacobs, P., 2008. Mapping volcano topography with remote sensing: ASTER vs SRTM. International Journal of Remote Sensing 29, 6515–6538. http://dx.doi.org/10.1080/01431160802167949.
Kiss, B., Harangi, Sz, Molnár, K., Ntaflos, T., 2011. The origin of dacite of the Csomád (Ciomadul) volcano (SE Carpathians, Eastern Central Europe). Soufrière Hills Volcano 15 Years On Conference, MVO, Montserrat, W.I., 4–8 April 2011.
Kristó, A., 1957. A Csiki-medencék geomorfológiai problémái (Geomorphic problems of the Ciuc Basin). in Hungarian Csiki Múzeum Közleményei (Annals of the Csiki Museum). Miercurea Ciuc (Csíkszereda), pp. 23–50.
Kristó, A., 1995. A Hargita felszínalaktani jellemvonásai (Geomorphological features of Hagrhita Mts.) : Földrajzi Közlemények (Bull. Hung. Geogr. Soc.), Budapest, 119 (43), pp. 11–21. in Hungarian with English abstract (1).
László, A., 2005. The post-Late Pontian paleogeographic evolution of the south Harghita Mountains area and the adjacent basins: Studia Universitatis Babeş-Bolyai, Geologia, Cluj, pp. 27–40.
Löbens, S., Bense, F.A., Wemmer, K., Dunkl, I., Costa, C.H., Layer, P., Siegesmund, S., 2011. Exhumation and uplift of the Sierras Pampeanas: preliminary implications from K-Ar fault gouge dating and low-T thermochronology in the Sierra de Comechingones (Argentina). International Journal of Earth Sciences 100, 671–694.
Lyman, A.W., Koenig, E., Fink, J.H., 2004. Predicting yield strengths and effusion rates of lava domes from morphology and underlying topography. Journal of Volcanology and Geothermal Research 129, 125–138.
Macías, J.L., Capra, J., Arce, J.L., Espíndola, J.M., García-Palomo, A., Sheridan, M.F., 2008. Hazard map of El Chichón volcano, Chiapas, México: Constraints posed by eruptive history and computer simulations. Journal of Volcanology and Geothermal Research 175, 444–458.
Magyari, E.K., Buczkó, K., Jakab, G., Braun, M., Szántó, Zs., Molnár, M., Pál, Z., Karátson, D., 2006. Holocene palaeohydrology and environmental history in the South Harghita Mountains, Romania: Földtani Közlöny (Bull. Hung. Geol. Soc.), Budapest, 136, pp. 249–284.
Magyari, E.K., Buczkó, K., Jakab, G., Braun, M., Pál, Z., Karátson, D., 2009. Palaeolimnology of the last crater lake in the Eastern Carpathian Mountains — a multiproxy study of Holocene hydrological changes. Hydrobiologia 631, 29–63.
Major, J.J., Dzurisin, D., Schilling, S.P., Poland, M.P., 2009. Monitoring lava-dome growth during the 2004–2008 Mount St. Helens, Washington, eruption using oblique terrestrial photography. Earth and Planetary Science Letters 286, 243–254.
Mason, P.R.D., Seghedi, I., Szakács, A., Downes, H., 1998. Magmatic constraints on geodynamic models of subduction in the Eastern Carpathians, Romania. Tectonophysics 297, 157–176.
McCanta, M.C., Rutherford, M.J., Hammer, J.E., 2007. Pre-eruptive and syn-eruptive conditions in the Black Butte, California dacite: insight into crystallization kinetics in a silicic magma system. Journal of Volcanology and Geothermal Research 160, 263–284.
McCurry, M., Hackett, W.R., Hayden, K., 1999. Cedar Butte and cogenetic rhyolite domes of the eastern Snake River Plain. In: Hughes, S.S., Thackray, G.D. (Eds.), Guidebook to the Geology of Eastern Idaho, Idaho Museum of Natural History, Idaho State University, Pocatello, ID, pp. 169–179.
Miailler, D., Boivin, P., Deniel, C., Gourgaud, A., Lanos, P., Sforna, M., Pilleyre, T., 2010. The ultimate summit eruption of Puy de Dôme volcano (Chaîne des Puys, French Massif Central) about 10,700 years ago. Comptes Rendus de l'Académie des Sciences, Geoscience 342, 847–854. http://dx.doi.org/10.1016/j.crte.2010.09.004 (E2-E3-E1).
Moriya, I., 1978. Morphology of lava domes. Bulletin of the Department of Geography Komazawa University of Japan 14, 55–69 (in Japanese).
Moriya, I., Okuno, M., Nakamura, T., Szakács, A., Seghedi, I., 1995. Last eruption and its 14C age of Ciomadul volcano, Romania. Summaries of Research Using AMS at Nagoya University, Dating and Materials Research Center 6, 82–91.
Moriya, I., Okuno, M., Nakamura, T., Ono, K., Szakács, A., Seghedi, I., 1996. Radiocarbon ages of charcoal fragments from the pumice flow deposit of the last eruption of Ciomadul volcano, Romania. Summaries of Research Using AMS at Nagoya University: Dating and Materials Research Center, 3, pp. 252–255.
Mureşan, M., Szakács, A., 1998. The Ciuc Formation: a Miocene prevolcanic detritic deposit east of the Harghita Mountains (East Carpathians). Révue Roumaine de Géologie, Bucharest 42, 7–27.
Myers, J.D., 1992. Herbert/Central Aleutian Islands. In: Wood, C.A., Kienle, J. (Eds.), Volcanoes of North America: The United States and Canada. Cambridge University Press (364 pp.).
Nakada, S., Miyake, Y., Sato, H., Oshima, O., Fujinawa, A., 1995. Endogenous growth of dacite dome at Unzen volcano (Japan), 1993–1994. Geology 23, 157–160.
Necea, D., 2010. High-resolution morpho-tectonic profiling across an orogen. Tectonic-controlled geomorphology and multiple dating approach in the SE Carpathians. PhD Thesis, VU University Amsterdam.

Ollier, C.D., 1988. Volcanoes. Basil Blackwell, Oxford (228 pp.).
Pál, Z., 2001. A Szent Anna-tó batimetriája (Bathymetry of Lake Saint Ana). Collegicum Geographicum, Babeş-Bolyai University, Cluj, 2, pp. 73–78. in Hungarian.
Pécskay, Z., Szakács, A., Seghedi, I., Karátson, D., 1992. Contributions to the geochronology of Mt. Cucu volcano and the South Harghita (East Carpathians, Romania). Földtani Közlöny (Bull. Hung. Geol. Soc.), Budapest, 122/2-4, pp. 265–286.
Pécskay, Z., Lexa, J., Szakács, A., Balogh, K., Seghedi, I., Konecny, V., Kovács, M., Márton, E., Kaliciak, M., Széky-Fux, V., Póka, T., Gyarmati, P., Edelstein, O., Rosu, E., Žec, B., 1995. Space and time distribution of Neogene-Quaternary volcanism in the Carpatho-Pannonian Region. Acta Vulcanologica 7 (2), 15–28.
Peltz, S., 1971. Contribuţii la cunoaşterea formaţiunii vulcanogen-sedimentare pleistocene din sudul munţilor Harghita şi nord-estul bazinului Baraolt (Contibution to the knowledge on the Pleistocene volcanogenic sedimentary formations from the S of Mt. Harghita to the NE of Baraolt basin). Dări de Seamă ale Şedinţelor, Institutul de Geologie si Geofizică Romania, LVII/5, pp. 173–189. in Romanian (Bucharest).
Peltz, S., Vajdea, E., Balogh, K., Pécskay, Z., 1987. Contribution to the Geochronological Study of the Volcanic Processes in the Calimani and Harghita Mts: Dari de Seama Inst. Geol. Romania, Bucharest, 72-73/1, pp. 323–338.
Popa, M., Radulian, M., Szakács, A., Seghedi, I., Zaharia, B., 2011. New seismic and tomography data in the Southern part of the Harghita Mountains (Romania, South-eastern Carpathians): connection with recent volcanic activity. Pure and Applied Geophysics. http://dx.doi.org/10.1007/s00024-011-0428-6 (published online).
Reid, M.R., Coath, C.D., 2000. In situ U–Pb ages of zircons from the Bishop Tuff: No evidence for long crystal residence times. Geology 28, 443–446.
Reimer, P.J., Baillie, M.G.L., Bard, E., Bayliss, A., Beck, J.W., Blackwell, P.G., Bronk Ramsey, C., Buck, C.E., Burr, G.S., Edwards, R.L., Friedrich, M., Grootes, P.M., Guilderson, T.P., Hajdas, I., Heaton, T.J., Hogg, A.G., Hughen, K.A., Kaiser, K.F., Kromer, B., McCormac, F.G., Manning, S.W., Reimer, R.W., Richards, D.A., Southon, J.R., Talamo, S., Turney, C.S.M., van der Plicht, J., Weyhenmeyer, C.E., 2009. IntCal09 and Marine09 radiocarbon age calibration curves, 0–50,000 years cal BP. Radiocarbon 51 (4), 1111–1150.
Reuter, H.I., Nelson, A., Strobl, P., Mehl, W., Jarvis, A., 2009. A First Assessment of ASTER GDEM Tiles for Absolute Accuracy, Relative Accuracy and Terrain Parameters: Proceedings 2009 IEEE International Geoscience and Remote Sensing Symposium (IGARSS), 5, pp. 240–243.
Santos, G.M., Southon, J.R., Griffin, S., Beaupre, S.R., Druffel, E.R.M., 2007. Ultra small-mass AMS ^{14}C sample preparation and analyses at KCCAMS/UCI Facility. Nuclear Instruments and Methods in Physics Research Section B 259, 293–302.
Schmitt, A.K., Grove, M., Harrison, T.M., Lovera, O., Hulen, J., Walters, M., 2003. The Geysers–Cobb Mountain Magma System, California (part 1): U–Pb zircon ages of volcanic rocks, conditions of zircon crystallization and magma residence times. Geochimica et Cosmochimica Acta 67 (18), 3423–3442.
Schreiber, W., 1972. Incadrarea geografica şi geneza Masivului Ciomadu (Geographic division and genesis of the Ciomadu Massif). Studia Universitatis Babeş-Bolyai, ser. Geographia, Cluj, 1, pp. 47–55. in Romanian with German abstract.
Seghedi, I., Downes, H., 2011. Geochemistry and tectonic development of Cenozoic magmatism in the Carpathian–Pannonian region. Gondwana Research 20, 655–672.
Seghedi, I., Downes, H., Harangi, S., Mason, P.R.D., Pécskay, Z., 2005. Geochemical response of magmas to Neogene-Quaternary continental collision in the Carpathian–Pannonian region: a review. Tectonophysics 410 (1–4), 485–499.
Shields, J., 2010. The morphometry of the Chaîne des Puys. MSc Thesis, Université Blaise Pascal, Clermont-Ferrand, 47 pp.
Stasiuk, M.V., Jaupart, C., 1997. Lava flow shapes and dimensions as reflections of magma system conditions. Journal of Volcanology and Geothermal Research 78 (1–2), 3 l-50.
Stuiver, M., Reimer, P.J., 1993. Extended C-14 Data-Base and Revised Calib 3.0 C-14 Age Calibration Program. Radiocarbon 35 (1), 215–230.
Szakács, A., Seghedi, I., 1986. Chemical diagnosis of the volcanics from the southeast-ernmost part of the Harghita Mountains — proposal for a new nomenclature. Revue Roumaine de Géologie 30, 41–48 (Bucharest).
Szakács, A., Seghedi, I., 1990. Quaternary dacitic volcanism in the Ciomadul massif (South Harghita Mts, East Carpathians, Romania). IAVCEI International Volcanological Congress, 3–8 Sept., Abstract Volume, Mainz.
Szakács, A., Seghedi, I., 1995. Time-space evolution of Neogene-Quaternary volcanism in the Calimani–Gurghiu–Harghita volcanic chain. Guide to excursion B3, IUGS, Regional committee on Mediteranean Neogene stratigraphy, Rom. Journal of Stratigraphy 76 (Suppl. 4) (Bucharest, 24 pp.).
Szakács, A., Seghedi, I., 1996. Volcaniclastic sequences around andesitic stratovolcanoes, East Carpathians, Romania. Joint field workshop of the IAVCEI Commissions on Explosive volcanism and volcanogenic sedimentation, August 25–September 1, 1996. Rom. Journal of Petrology 77 (1) (Bucharest, 55 pp.).
Szakács, A., Seghedi, I., Pécskay, Z., 1993. Pecularities of South Harghita Mts. as the terminal segment of the Carpathian Neogene to Quaternary volcanic chain. Revue Roumaine de Géologie, Géophysique et Géographie. Série de Géologie 37, 21–36 (Bucharest).
Szakács, A., Ioane, D., Seghedi, I., Rogobete, M., Pécskay, Z., 1997. Rates of migration of volcanic activity and magma output along the Calimani–Gurghiu–Harghita volcanic range, East Carpathians, Romania. Przeglad Geologiczny: PANCARDI meeting abstracts, 45, p. 1106 (10).
Szakács, A., Seghedi, I., Pécskay, Z., 2002. The most recent volcanism in the Carpathian–Pannonian region. Is there Any Volcanic Hazard? Geologica Carpathica Special Issue, Proceedings of the XVIIth Congress of Carpatho-Balkan Geological Association, 53, pp. 193–194.
Székely, A., 1957. Az Erdélyi vulkanikus hegységek geomorfológiai problémái (Geomorphological Problems of the Volcanic Mountains Of Transylvania). Földrajzi Értesítő (Bull. Hung. Geogr. Soc.), Budapest, 57, pp. 235–259. In Hungarian.
Tanguy, J.-C., 2004. Rapid dome growth at Montagne Pelee during the early stages of the 1902–1905 eruption: a reconstruction from Lacroix's data. Bulletin of Volcanology 66, 615–621.
Tantau, I., Reille, M., de Beaulieu, J.L., Farcas, S., Goslar, T., Paterne, M., 2003. Vegetation history in the eastern Romanian Carpathians: pollen analysis of two sequences from the Mohos crater. Vegetation History and Archaeobotany 12, 113–125.
Tarquini, S., Isola, I., Favalli, M., Mazzarini, F., Bisson, M., Pareschi, M.T., Boschi, E., 2007. TINITALY/01: a new triangular irregular network of Italy. Annals of Geophysics 50, 407–425.
Thouret, J.-C., 1999. Volcanic geomorphology — an overview. Earth-Science Reviews 47, 95–132.
Vaselli, O., Minissale, A., Tassi, F., Magro, G., Seghedi, I., Ioane, D., Szakács, A., 2002. A geochemical traverse across the Eastern Carpathians (Romania): constraints on the origin and evolution of the mineral water and gas discharges. Chemical Geology 182, 637–654.
Veres, D., Davies, S.M., Wohlfarth, B., Preusser, F., Wastegard, S., Ampel, L., Hormes, A., Possnert, G., Raynal, J.-P., Vernet, G., 2008. Age, origin and significance of a new middle MIS 3 tephra horizon identified within a long-core sequence from Les Echets, France. Boreas 37, 434–443.
Veres, D., Lallier-Vergès, E., Wohlfarth, B., Lacourse, T., Kéravis, D., Björck, S., Preusser, F., Andrieu-Ponel, V., Ampel, L., 2009. Climate-driven changes in lake conditions during MIS 3 and 2: a high-resolution geochemical record from Les Echets, France. Boreas 38, 230–243.
Vinkler, A.P., Harangi, Sz, Ntaflos, T., Szakács, A., 2007. A Csomád vulkán (Keleti-Kárpátok) horzsaköveinek kőzettani és geokémiai vizsgálata — petrogenetikai következtetések (Petrology and geochemistry of the pumices from the Ciomadul volcano [Eastern Carpathians] — implications for the petrogenetic processes). Földtani Közlöny (Bull. Hung. Geol. Soc.), Budapest, 137, pp. 103–128.
Volcanic Hazard Report for Southern Dominica, 2000. The University of West Indies, Seismic Research Unit, 49 pp.
Watts, R.B., Herd, R.A., Sparks, R.S.J., Young, S.R., 2002. Growth patterns and emplacement of the andesitic lava dome at the Soufrière Hills Volcano. In: Druitt, T.H., Kokelaar, B.P. (Eds.), The eruption of Soufrière Hills Volcano, Montserrat, from 1995 to 1999: Geological Society London Memoir.
Wood, C.A., 1980. Morphometric evolution of cinder cones. Journal of Volcanology and Geothermal Research 7, 387–413.
Wright, R., Garbeil, H., Baloga, S.M., Mouginis-Mark, P.J., 2006. An assessment of shuttle radar topography mission digital elevation data for studies of volcano morphology. Remote Sensing of Environment 105, 41–53. http://dx.doi.org/10.1016/j.rse.2006.06.002.
Zimbelman, J.R., Fagents, S.A., Gregg, T.K.P., Manley, C.R., Rowland, S.K., 2000. Subaerial terrestrial volcanism: eruptions in our own backyard. In: Zimbelman, J.R., Gregg, T.K.P. (Eds.), Environmental Effects on Volcanic Eruptions: From Deep Oceans to Deep Space. Kluwer Academic/Plenum Publishers, New York, pp. 9–38.